

On Mass Bands in the Crystal Manifold

R.I. de Oliveira Junior^{a1}, G. Alencar^{a2}, R.R. Landim^{a3} and R.N. Costa Filho^{a4}

^a*Departamento de Física, Universidade Federal do Ceará- Caixa Postal 6030, Campus do Pici, 60455-760, Fortaleza, Ceará, Brazil.*

Abstract

In this paper, we revisit two results that consider a crystal manifold background in the Randall-Sundrum scenario (RS) and add the discussion related to geometrical couplings in such a configuration. The wave functions of fields trapped in the crystal are Bloch-like waves, and their behavior is very similar to electrons inside a lattice, just like in the Kronig-Penney model (KP). We compute the mass dispersion relation for those fields with and without a dilaton coupling. We find that this relation is very different from the one obtained in previous works. It leads to new results for the band gap structure of these fields. The most important consequence is that the mass gap for gravity differ by two order of magnitude from the previous results of the literature. In the case of the Kalb-Ramond field, and with the correct dispersion relation, there is no gap between the mass bands. When the generalization to the q-form is done, we show that it is not possible to suppress or generate mass for the fields by controlling the dilaton coupling, differently of what was argued in one of the works revised. When regarding the geometrical coupling, we find some similarities (the gauge and Kalb-Ramond, with both couplings, has the same dispersion as the free scalar and gravitational fields) and some differences (the order of the Bessel's function in the dispersion relations changes, if we consider one coupling per time). We also calculate the mass for the first mass mode for each field studied. Where we found, for example, a massive photon with a mass of order $10^{-31} kg$.

¹e-mail: ivan@fisica.ufc.br

²e-mail: geova@fisica.ufc.br

³e-mail: renan@fisica.ufc.br

⁴e-mail: rai@fisica.ufc.br

1 Introduction

When electrons move inside solids, they experience a potential due to the ions in the lattice. Therefore the electrons are subject to a periodic potential inside the lattice. The simplest way to describe this system is the Kronig-Penney model [1] which is based on Bloch's idea [2]: the interaction of the electron with the particles in an one dimensional crystal can be approximated by a periodic potential. By solving the Schrödinger equation with that potential, one can find the allowed energy of the system. In fact, this is one of the few models of quantum mechanics in which the eigenvalues and eigenfunctions of the energy can be found analytically. More than this, the model also provides analytic expressions for the dispersion relation. With this at hand, it is possible to find that some values of the energy are not allowed, called the band gap. Thus, the Kronig-Penney can be considered as one of the simplest models exhibiting a band gap. This kind of behavior has important consequences in condensed matter, in the computation of the conductivity, for example.

The use of condensed matter tools to study physics of membranes is not new. The fact is that, in the last years, the models in physics of extra dimensions brought back to the arena the analysis of the Schroedinger equation. In these models, the interaction between the several fields and the membrane is an important aspect to be understood. Localization procedures, for example, have been studied since the Randall-Sundrum model [3, 4] was presented. Many proposals were made pursuing to localize fields of different spins in several membrane structures [5–17]. All of these problems can be studied using Schrödinger like equations. One interesting point about the trapping of fields is that the massive modes are never localized. The reason is that the solutions to the Schroedinger equation are plane waves in the extra dimension and therefore propagate in this direction. However the massive modes can have peaks of probability over the brane and show up as resonances. Therefore, the structure of resonances can tell us about unstable modes that in principle could be measured at the brane [16–25]. With the condensed matter analogy in mind, some of the present authors applied the transfer matrix method to compute resonances [26–28]. This was possible since particles moving through the extra dimensions resembles the wave packets of electrons hitting the potential barriers inside semiconductors.

Beyond semiconductors, the next analogy is that of a periodic crystal. This construction, in the extra dimensions scenario with many branes, was presented in Ref. [29] and was called crystal manifold universe. The author found brane-world solutions regarding intersecting families of parallel $n + 2$ -branes in a $4 + n$ -dimensional AdS space. Soon latter other generalizations were considered [30–35]. In these models, there are branes in any direction of the bulk, and they can have intersections. These works gave rise to discussions related to, for example, cosmological braneworld models [36, 37] and dark matter [38, 39]. Yet in Ref. [29], the authors applied his general construction for the gravitational field in such a background. The main difference between this model and RS II (with just one brane) is that now the massive modes can appear as stable

ones over the brane. To be more precise, as in the Kronig-Penney model, they found a dispersion relation that gave the allowed values of mass, generating a band gap structure. With this, it was proposed to compute the correction to the Newton's law by

$$V \approx -G \frac{m_1 m_2}{r} + \int_{m_{gap}}^{\infty} \frac{dm}{K} \frac{G m_1 m_2}{r} \frac{m}{K} e^{-mr}. \quad (1)$$

Finally, the authors gave an heuristic estimation of the first mass gap. The mass found by them was $m_{gap} = \frac{\mathcal{O}(1)}{l+L}$, where L is the AdS curvature and l the distance between the branes.

In the case of a D-dimensional universe, there is the possibility of the existence of many antisymmetric fields [40]. However, in five dimensions, the relevant ones are the one, two and three forms. This happens because of the counting of physical degrees of freedom, and also because they are canceled out in the visible brane due to the gauge freedom. The new field that appear, for instance, the 2-form, is important because it may be related, for example, to the spacetime torsion or the axion field [41–43]. The mass spectrum of the two and three forms are also studied in [41, 44]. These fields appear naturally in string theory and have a relation with the ADS/CFT conjecture [45–47]. With this in mind, in Ref. [35], the authors extended the above results and considered other fields in the crystal manifold, namely the scalar, gauge, Kalb-Ramond and q-form fields, with and without the dilaton coupling (a scalar field used in order to localize the gauge field in a thick brane [5]). They found numerically the structure of the mass bands for all the fields, including gravity.

However, in reviewing the basic results related to crystal manifold universes, we found mistakes in the computation of the dispersion relation for the gravitational field found in [29]. Beyond this, since we have mass bands, it should be clear that the correct expression for the correction to the Newton's Law is given by

$$V \approx -G \frac{m_1 m_2}{r} + \sum_i \int_{m_i}^{M_i} \frac{dm}{K} \frac{G m_1 m_2}{r} \frac{m}{K} e^{-mr}, \quad (2)$$

where $[m_i, M_i]$ are the intervals of allowed mass. With the new dispersion relation we show numerically that the structure of the mass bands is completely different. For example, we find that we have a band in the interval $[0, M_1]$. We also find that the correct value of M_1 is two orders of magnitude fewer than the one proposed heuristically in Ref. [29]. Therefore this provides a very different phenomenology for the model. Finally, since the same expression was used for other fields in Ref. [35], we also revisit the mass band for q-form fields. Beyond this, as new models, we also study the influence of the geometrical coupling in the mass band of these fields. The geometrical coupling is a technique developed to localize q-form fields. The localization is done through the coupling with the Ricci scalar or Ricci tensor, as can be seen in [7, 10, 48–51]. We study here the gauge, Kalb-Ramond and q-form fields with both couplings. With that at hand, we generate new band gap structures different from the case with dilaton coupling.

The organization of this work is as follows. In section two we review the crystal manifold universe. Section three is devoted to the review of the gravitational case. The development of the general dispersion relation is done in the fourth section. In section five, we calculate the parameters for all the fields that we deal with: scalar, gravitational, gauge, Kalb-Ramond and q-forms. The study with geometrical coupling is done in section six. Finally, we present our conclusions and perspectives of future works.

2 Review of the Crystal Manifold Background

In this section we make a brief review of the crystal manifold background. A discussion with more details can be found at [29]. The crystal manifold is described by an array of $2+n$ -branes in a $4+n$ -dimensional AdS space, equally distant and with same brane tension. The action describing such a configuration is

$$S = \int_M d^{4+n}x \sqrt{g_{4+n}} \left(\frac{R}{2\kappa_{4+n}^2} + \Lambda \right) - \sum_{k=1}^n \sum_{j_k} \int_{j_k l_k} d^{3+n}x \sqrt{g_{3+n}} \sigma_k. \quad (3)$$

Where $\kappa_{4+n}^2 = \frac{8\pi}{M_*^{n+2}}$, and M_* is the fundamental scale of the theory. The equation of motion from (3) is

$$G_N^M = \kappa_{4+n}^2 \Lambda \delta_N^M - \sum_{k=1}^n \frac{\sqrt{g_{3+n}}}{\sqrt{g_{4+n}}} |k \kappa_{4+n}^2 \sigma_k \sum_j (-1)^j \delta(z^k - j l_k) \text{diag}(1, 1, 1, 1, 1, \dots, 0_k, \dots, 1). \quad (4)$$

Where z^k parameterize the extra dimensions.

The general solution that is valid in the whole manifold (bulk and branes) is written in the form

$$ds_{n+4}^2 = \Omega^2 (\eta_{\mu\nu} dx^\mu dx^\nu + \sum_{k=1}^n (dz^k)^2), \quad (5)$$

where n is the number of spatial extra dimensions. The solution for the conformal factor Ω is

$$\Omega^{-1} = K \sum_{k=1}^n \mathcal{S}(z^k) + 1, \quad (6)$$

with $K = (\sqrt{n}L)^{-1}$ and the functions \mathcal{S} satisfying

$$\begin{aligned} \frac{d^2 \mathcal{S}(z^k)}{d(z^k)^2} &= 2 \sum_j (-1)^j \delta(z^k - j l_k), \\ \left| \frac{d\mathcal{S}(z^k)}{dz^k} \right| &= 1. \end{aligned} \quad (7)$$

Here L is the AdS radius, and l_k the separation of the branes. The function \mathcal{S} which solves (7) is the sawtooth function, that can be written as follow

$$\mathcal{S}(z^k) = \begin{cases} \dots \\ 2pl_k - z^k, & \text{for } (2p-1)l_k < z^k < 2pl_k; \\ z^k - 2pl_k, & \text{for } 2pl_k < z^k < (2p+1)l_k; \\ \dots \end{cases} . \quad (8)$$

In this manuscript we will deal only with one extra dimension, i.e., $n = 1$. This means that we will work in the 5-dimensional case. In order to get the set of equations that we will deal with, we just put $n = 1$ in the previous group of equations.

Here, like in [5, 28], we will also analyze the cases with the dilaton coupling. The metric in this configuration reads

$$ds^2 = e^{2A(y)}\eta_{\mu\nu}dx^\mu dx^\nu + e^{2B(y)}dy^2. \quad (9)$$

By solving the Einstein's equations with this metric one gets

$$B(y) = \frac{A(y)}{4}, \quad \pi = -\sqrt{3M^3}A(y). \quad (10)$$

In [35], the authors introduced a parameter b so that $B(y) = (1 - b)A(y)$. If $b = \frac{3}{4}$ the dilaton is introduced together with its consequences. When $b = 1$ the dilaton coupling disappear. They also introduced the transformation $\frac{dy}{dz} = e^{A(y)-B(y)} = e^{bA(y)} = \Omega(z)$ to be performed in (9), in order to obtain a conformal metric like (5). The transformation leads to $\bar{A}(z) = \ln \Omega(z)/b$, where $A(y) = \bar{A}(z)$.

3 Revisiting the Gravitational Case

In the previous section we revised the crystal manifold background. In this one we will review the dispersion relation found by [29] and [35]. We will show that this dispersion relation is not correct, leading to wrong band gap structure for the mass. After that, we show, clearly, how to get the right dispersion relation, as well as the new results.

3.1 The Wrong Dispersion Relation

When treating the gravitational field, we are interested in linear perturbations of the 4D metric of the form $\bar{g}_{\mu\nu} = g_{\mu\nu} + h_{\mu\nu}$ [29]. Where $h_{\mu\nu}$ are the fluctuations in the transverse traceless gauge: $\nabla_\mu h_\nu^\mu = h_\nu^\mu = 0$. In first order, the perturbation satisfy

$$\delta R_{\mu\nu} = \frac{1}{2}R_\nu^\lambda h_{\mu\lambda} + \frac{1}{2}R_\mu^\lambda h_{\lambda\nu}. \quad (11)$$

Substituting the background metric (5) with $n = 1$, and defining the wave function $h_{\mu\nu} = \Omega\Psi$, where Ψ is a complex function that is formed by linear combination of $+$ and x polarizations, the authors in [29] found a Schrödinger like equation

$$\Psi'' + \left(m^2 - \frac{15}{4(\mathcal{S}(z) + L)^2} \right) \Psi + \frac{3}{\mathcal{S}(z) + L} \sum_j (-1)^j \delta(z - jl) \Psi = 0. \quad (12)$$

As claimed in [29] this is similar to a Schrödinger equation of an electron in a periodic potential, which assembles the Kronig-Penney (KP) model [1].

The technics used by them to solve (12) is similar to the (KP) model. Since the metric is periodic, they choose two elementary cells where the Schrödinger equation is solved. They chose the cells between $0 < z < 2l$ and $2l < z < 4l$. Because the presence of the delta function in (12), the boundary conditions for the functions are continuous while the boundaries conditions for the derivative are not. In the vertex l and $2l$ they are: $\Psi'(l_+) - \Psi'(l_-) = \frac{3}{l+L}\Psi(l)$, $\Psi'(2l_+) - \Psi'(2l_-) = -\frac{3}{L}\Psi(2l)$, $\Psi(l_+) = \Psi(l_-)$ and $\Psi(2l_+) = \Psi(2l_-)$. Solving the Schrödinger equation for these two elementary cells with the help of the boundaries conditions, they find the following dispersion relation

$$\cos(lq) = \frac{(j_2 n_1 + j_1 n_2)(\hat{j}_2 \hat{n}_1 + \hat{j}_1 \hat{n}_2) - \hat{j}_1 \hat{j}_2 (j_1 j_2 + 3n_1 n_2)}{2(j_2 n_1 - j_1 n_2)(\hat{j}_2 \hat{n}_1 - \hat{j}_1 \hat{n}_2)} - \frac{\hat{n}_1 \hat{n}_2 (3j_1 j_2 + n_1 n_2)}{2(j_2 n_1 - j_1 n_2)(\hat{j}_2 \hat{n}_1 - \hat{j}_1 \hat{n}_2)}. \quad (13)$$

In $q = 0$ there is a gap in the spectrum of mass given by the equation

$$\begin{aligned} j_1 j_2 \hat{j}_1 \hat{j}_2 + n_1 n_2 \hat{n}_1 \hat{n}_2 + j_2 \hat{j}_2 \hat{n}_1 n_1 + j_1 \hat{j}_1 n_2 \hat{n}_2 = \\ 3j_1 \hat{j}_2 \hat{n}_1 n_2 + 3\hat{j}_1 j_2 n_1 \hat{n}_2 - 3\hat{j}_1 \hat{j}_2 n_1 n_2 - 3j_1 j_2 \hat{n}_1 \hat{n}_2. \end{aligned} \quad (14)$$

This equation provides a constraint in m . Solving it gives us the lowest value of mass, and consequently the magnitude of the gap. The authors in [29], does not solve this equation explicit. What they do is just analyze the arguments of the Bessel functions that are mL and $m(l+L)$. Then, they argue that the only two candidates for the mass gap (m_{gap}) are L^{-1} and $(l+L)^{-1}$. The first option is excluded, because that in the limit of $l \rightarrow \infty$ the single brane case [4] must be satisfied. Then the mass gap must be

$$m_{gap} = \frac{\mathcal{O}(1)}{l+L}. \quad (15)$$

In the next subsection, we will show that the result (13) is not right, as well as the equation (14). We also calculate the explicit value of the numerator in (15), finding a bigger correction to Newton's law.

3.2 The Correct Dispersion Relation

Now we present the way that we calculated the dispersion relation for the gravitational case, which means that we start from equation (12). As in [29], we use

the analogy of electrons inside a crystal, that way we need to solve(12) for two adjacent elementary cells. Solving for these two cells it is possible to relate the constants in the wave functions in order to obtain the dispersion relation. The procedure that we will use is based on the transfer matrix technics, also used in [35].The configuration for the two elementary cells can be seen in the figure below

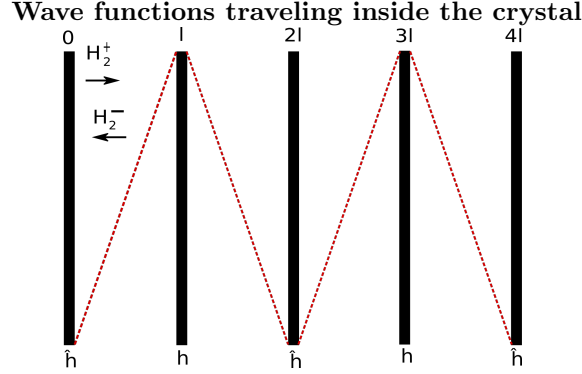


Figure 1: One patch of the 1-D crystal (Two adjacent cells)

To calculate the boundaries conditions to (12) we have to realize that $\mathcal{S}(z) = l$ for $z = l, 3l, 5l, \dots$ and $\mathcal{S}(z) = 0$ for $z = 0, 2l, 4l, \dots$. Calculating the condition in $z = l$ and $j = 1$, we have

$$\Psi'(l^+) - \Psi'(l^-) = \frac{3\Psi(l)}{(l+L)}. \quad (16)$$

And for $z = 2l$ and $j = 2$, we find

$$\Psi'(2l^+) - \Psi'(2l^-) = -\frac{3}{L}\Psi(2l). \quad (17)$$

Once that the wave function has no discontinuity, its boundaries conditions are

$$\Psi(l^+) = \Psi(l^-) \quad \text{and} \quad \Psi(2l^+) = \Psi(2l^-). \quad (18)$$

The differential equation for the first cell can be written as

$$\Psi'' + m^2\Psi = \begin{cases} \frac{15}{4(z+L)^2}\Psi & p/ & 0 < z < l \\ \frac{15}{4(2l-z+L)^2}\Psi & p/ & l < z < 2l \end{cases}. \quad (19)$$

The above equations can be transformed in a standard Bessel equation through the transformation

$$\Psi = \begin{cases} \sqrt{u}\Psi(u) & u = m(z+L) & p/ & 0 < z < l \\ \sqrt{v}\Psi(v) & v = m(2l-z+L) & p/ & l < z < 2l \end{cases}. \quad (20)$$

After doing the derivatives in (20), and substituting in (19), we found

$$\begin{cases} u^2\Psi''(u) + u\Psi'(u) + [u^2 - 4]\Psi(u) = 0 & u = m(z + L) & \text{for } 0 < z < l \\ v^2\Psi''(v) + v\Psi'(v) + [v^2 - 4]\Psi(v) = 0 & v = m(2l - z + L) & \text{for } l < z < 2l \end{cases} \quad (21)$$

We then see that $\nu = 2$. This is the order of the Bessel functions that we will consider from now on.

The solution for the first cell is given by

$$\Psi = \begin{cases} \sqrt{u}(AH_2^+(u) + BH_2^-(u)) & 0 < z < l & u = m(z + L) \\ \sqrt{v}(CH_2^+(v) + DH_2^-(v)) & l < z < 2l & v = m(2l - z + L). \end{cases} \quad (22)$$

Where H_2^\pm are the Hankel functions of first and second kind of order two. They are defined as

$$H_2^+ = J_2 + iN_2 \quad \text{and} \quad H_2^- = J_2 - iN_2. \quad (23)$$

with J_2 and N_2 being the Bessel functions of first and second kind and order two. To simplify the solution (22), we define the quantities

$$\begin{cases} E(u) = \sqrt{u}H_2^+(u) \\ F(u) = \sqrt{u}H_2^-(u) \\ G(v) = \sqrt{v}H_2^+(v) \\ I(v) = \sqrt{v}H_2^-(v) \end{cases}, \quad (24)$$

then equation (22) becomes

$$\Psi = \begin{cases} AE(u) + BF(u) & 0 < z < l & u = m(z + L) \\ CG(v) + DI(v) & l < z < 2l & v = m(2l - z + L) \end{cases}. \quad (25)$$

It is important to not that in the vertex $z = l$ we have

$$\begin{cases} E(l) = G(l) \\ F(l) = I(l) \\ E'(l) = G'(l) \\ F'(l) = I'(l). \end{cases} \quad (26)$$

By using (26) and the boundaries conditions for the function and its derivative in $z = l$, we get

$$\begin{pmatrix} E(l) & F(l) \\ -mE'(l) & -mF'(l) \end{pmatrix} \begin{pmatrix} C \\ D \end{pmatrix} = \begin{pmatrix} E(l) & F(l) \\ mE'(l) + \frac{2cE(l)}{(l+L)} & mF'(l) + \frac{2cF(l)}{(l+L)} \end{pmatrix} \begin{pmatrix} A \\ B \end{pmatrix}. \quad (27)$$

Where $E'(l) = \frac{dE(u)}{du}|_{z=l}$ and $F'(l) = \frac{dF(u)}{du}|_{z=l}$. With this matrix we can relate the constants C and D with A and B . It is valid to mention that when we derive the Hankel functions we use the relation $\frac{dH^\pm}{du} = H_1^\pm - \frac{2}{u}H_2^\pm$. Also, we use the following definitions in the vertex $H_{1,2}^\pm(0) = H_{1,2}^\pm(2l) = H_{1,2}^\pm(4l) = \hat{h}_{1,2}^\pm$ (for all l even) and $H_{1,2}^\pm(l) = H_{1,2}^\pm(3l) = h_{1,2}^\pm$ (for all l odd), where $h_1^\pm = j_1 \pm in_1$ and $h_2^\pm = j_2 \pm in_2$. The same definition applies to $\hat{h}_{1,2}^\pm$, but with $\hat{j}_{1,2}$ and $\hat{n}_{1,2}$. When we explicit the constants C, D , we have

$$\begin{pmatrix} C \\ D \end{pmatrix} = \begin{pmatrix} -\frac{(h_2^- h_1^+ + h_2^+ h_1^-)}{h_2^- h_1^+ - h_2^+ h_1^-} & -\frac{2h_2^- h_1^-}{h_2^- h_1^+ - h_2^+ h_1^-} \\ \frac{2h_2^+ h_1^+}{h_2^- h_1^+ - h_2^+ h_1^-} & \frac{(h_2^- h_1^+ + h_2^+ h_1^-)}{h_2^- h_1^+ - h_2^+ h_1^-} \end{pmatrix} \begin{pmatrix} A \\ B \end{pmatrix} = K \begin{pmatrix} A \\ B \end{pmatrix}. \quad (28)$$

The wave function for the first cell is

$$\Psi = \begin{cases} \sqrt{m(z+L)}[AH_2^+(m(z+L)) + BH_2^-(m(z+L))] & 0 < z < l \\ \sqrt{m(2l-z+L)} \left[\left(-\frac{(h_2^- h_1^+ + h_2^+ h_1^-)}{h_2^- h_1^+ - h_2^+ h_1^-} A - \frac{2h_2^- h_1^-}{h_2^- h_1^+ - h_2^+ h_1^-} B \right) H_2^+(m(2l-z+L)) \right. \\ \left. + \left(\frac{2h_2^+ h_1^+}{h_2^- h_1^+ - h_2^+ h_1^-} A + \frac{(h_2^- h_1^+ + h_2^+ h_1^-)}{h_2^- h_1^+ - h_2^+ h_1^-} B \right) H_2^-(m(2l-z+L)) \right] & l < z < 2l. \end{cases} \quad (29)$$

For the other cell the procedure is similar, and we get

$$\Psi = \begin{cases} \sqrt{m(z-2l+L)}[\hat{A}H_2^+(m(z-2l+L)) + \hat{B}H_2^-(m(z-2l+L))] & 2l < z < 3l \\ \sqrt{m(4l-z+L)} \left[\left(-\frac{(h_2^- h_1^+ + h_2^+ h_1^-)}{h_2^- h_1^+ - h_2^+ h_1^-} \hat{A} - \frac{2h_2^- h_1^-}{h_2^- h_1^+ - h_2^+ h_1^-} \hat{B} \right) H_2^+(m(4l-z+L)) \right. \\ \left. + \left(\frac{2h_2^+ h_1^+}{h_2^- h_1^+ - h_2^+ h_1^-} \hat{A} + \frac{(h_2^- h_1^+ + h_2^+ h_1^-)}{h_2^- h_1^+ - h_2^+ h_1^-} \hat{B} \right) H_2^-(m(4l-z+L)) \right] & 3l < z < 4l. \end{cases} \quad (30)$$

For each cell we have the wave function depending on just two constants, we then have to relate them. To do it, we use the Boundaries condition for the Bloch wave ¹ together with the usual conditions

$$\begin{cases} \Psi(2l) = e^{2iqL}\Psi(0) \\ \Psi(4l) = e^{2iqL}\Psi(2l) \\ \Psi(2l^+) = \Psi(2l^-) \\ \Psi'(2l^+) - \Psi'(2l^-) = -\frac{3}{L}\Psi(2l). \end{cases} \quad (31)$$

Using the first condition in (31), and the equation (28), we have

$$B = \frac{(e^{2iqL}\hat{h}_2^+ - \hat{h}_2^+ K_{11} - \hat{h}_2^- K_{21})A}{\hat{h}_2^+ K_{12} + \hat{h}_2^- K_{22} - e^{2iqL}\hat{h}_2^-}. \quad (32)$$

For the second cell, and using the second condition in (31)

$$\hat{B} = \frac{(e^{2iqL}\hat{h}_2^+ - \hat{h}_2^+ K_{11} - \hat{h}_2^- K_{21})\hat{A}}{\hat{h}_2^+ K_{12} + \hat{h}_2^- K_{22} - e^{2iqL}\hat{h}_2^-}. \quad (33)$$

¹ $\psi(z_i + 2l) = e^{2iqL}\psi(z_i)$

We yet define

$$f = \frac{(e^{2iql}\hat{h}_2^+ - \hat{h}_2^+K_{11} - \hat{h}_2^-K_{21})}{\hat{h}_2^+K_{12} + \hat{h}_2^-K_{22} - e^{2iql}\hat{h}_2^-}, \quad (34)$$

which allows us to write (32) and (33) as $B = fA$ and $\hat{B} = f\hat{A}$. The third condition in (31) leads to

$$\hat{A} = e^{2iql}A. \quad (35)$$

Then we have four constants and three equations; (32),(33) and (35). The other equation that we need is found by using the last condition in (31), and using a similar procedure that we did to find the transfer matrix through the vertex l , the result is

$$\begin{pmatrix} \hat{A} \\ \hat{B} \end{pmatrix} = \begin{pmatrix} -\frac{(\hat{h}_2^- \hat{h}_1^+ + \hat{h}_2^+ \hat{h}_1^-)}{\hat{h}_2^- \hat{h}_1^+ - \hat{h}_2^+ \hat{h}_1^-} & -\frac{2\hat{h}_2^- \hat{h}_1^-}{\hat{h}_2^- \hat{h}_1^+ - \hat{h}_2^+ \hat{h}_1^-} \\ \frac{2\hat{h}_2^+ \hat{h}_1^+}{\hat{h}_2^- \hat{h}_1^+ - \hat{h}_2^+ \hat{h}_1^-} & \frac{(\hat{h}_2^- \hat{h}_1^+ + \hat{h}_2^+ \hat{h}_1^-)}{\hat{h}_2^- \hat{h}_1^+ - \hat{h}_2^+ \hat{h}_1^-} \end{pmatrix} \begin{pmatrix} C \\ D \end{pmatrix} = \hat{K} \begin{pmatrix} C \\ D \end{pmatrix}. \quad (36)$$

Here \hat{K} is the same matrix than K , but with $h \rightarrow \hat{h}$. Placing (31),(32),(33) and (35) in (36),we get

$$\begin{pmatrix} e^{2iql} \\ fe^{2iql} \end{pmatrix} = \hat{K}K \begin{pmatrix} 1 \\ f \end{pmatrix}. \quad (37)$$

Until now our procedure assembles the ones used in [29] and [35].However, there it is not very clear how they arrive in the dispersion relation starting from equation (37). What we do now is to show how to solve this equation in a very simple way. The equation above can yet be written as

$$\begin{pmatrix} e^{2iql} - (\hat{K}_{11}K_{11} + \hat{K}_{12}K_{21}) & -(\hat{K}_{11}K_{12} + \hat{K}_{12}K_{22}) \\ -(\hat{K}_{11}K_{12} + \hat{K}_{12}K_{22}) & e^{2iql} - (\hat{K}_{21}K_{12} + \hat{K}_{22}K_{22}) \end{pmatrix} \begin{pmatrix} 1 \\ f \end{pmatrix} = 0 \quad (38)$$

The above equation has solution if the determinant of the matrix that multiply $\begin{pmatrix} 1 \\ f \end{pmatrix}$ be equal to zero, i.e.,

$$e^{4iql} - e^{2iql}[(\hat{K}_{21}K_{12} + \hat{K}_{22}K_{22}) + (\hat{K}_{11}K_{11} + \hat{K}_{12}K_{21})] + (\hat{K}_{11}K_{11} + \hat{K}_{12}K_{21}).(\hat{K}_{21}K_{12} + \hat{K}_{22}K_{22}) - (\hat{K}_{11}K_{12} + \hat{K}_{12}K_{22}).(\hat{K}_{21}K_{11} + \hat{K}_{22}K_{21}) = 0. \quad (39)$$

It can be written as

$$e^{4iql} - e^{2iql}\text{Tr}(\hat{K}K) + \det(\hat{K}K) = 0. \quad (40)$$

Using (28) and (36),it is straightforward to show that $\det(\hat{K}K) = 1$. Then,using the fact that $\det(\hat{K}K) = 1$, from (40) we get

$$\cos(2ql) = \frac{1}{2}\text{Tr}(\hat{K}K). \quad (41)$$

Coming back with the definitions of h_1^\pm and h_2^\pm and putting in terms of $\cos(ql)$, we have

$$\cos(ql) = \sqrt{\frac{-\hat{j}_1\hat{j}_2n_1n_2 - \hat{n}_1\hat{n}_2j_1j_2 + \hat{j}_2\hat{n}_1j_2n_1 + \hat{j}_1\hat{n}_2j_1n_2}{(\hat{j}_2\hat{n}_1 - \hat{j}_1\hat{n}_2)(j_2n_1 - j_1n_2)}}. \quad (42)$$

It is clear that this dispersion is very different of (13). Then we felt the need to review the works [29] and [35]. We will now show the results that we found using our dispersion relation, and compare with the old ones.

In order to do the numerical calculations, we need to give the magnitude of some parameters. If we want to have gravity in the observational bound, the relation between l and L is $\frac{l^3}{L^2} \leq 1mm$ [29]. And $M_{PL}^2 \approx M_*^3LN$. N is the number of branes in the crystal. The fundamental scale satisfy $M_* \approx \frac{1}{L} * TeV$ and, if we take $l \approx eV^{-1} \ll 1mm$, we find $N \approx 10^{16}$, $M_* \approx 100TeV(\frac{1}{L} \approx 100)$. In (42), we have also used as the argument of the Bessel functions

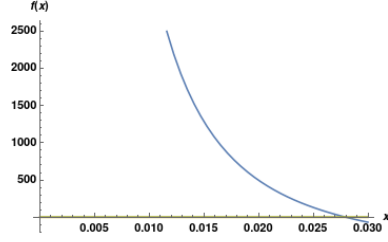
$$\begin{aligned} \hat{n}_2 &= N_2(mL) \\ \hat{n}_1 &= N_1(mL) \\ n_2 &= N_2(m(l+L)) \\ n_1 &= N_1(m(l+L)) \end{aligned} \quad (43)$$

and

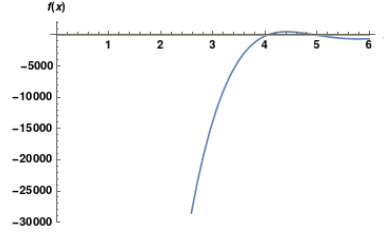
$$\begin{aligned} \hat{j}_2 &= J_2(mL) \\ \hat{j}_1 &= J_1(mL) \\ j_2 &= J_2(m(l+L)) \\ j_1 &= J_1(m(l+L)). \end{aligned} \quad (44)$$

With l being the distance between the branes, and L the AdS radius.

When we calculate the limit of (42) with $m \rightarrow 0$, we find that the dispersion relation tends smoothly to one. This means that the first band of mass starts at zero in ($ql \approx 0$) and goes until a maximum value in $ql = 0.5\pi$, as can be seen in Figure3. To find this maximum we plot (42) for $ql = 0.5\pi$. Here, contrarily of [29], we find the exact value of this first mode. In [29], the author just gave an heuristic estimation of this mass, suggested to be given by $m_{gap} = \mathcal{O}(1)/(l+L)$. By an explicit calculation we find that this numerator, using their wrong expression, is in fact 4. Let us see the plot for the first mode for both dispersion relation.



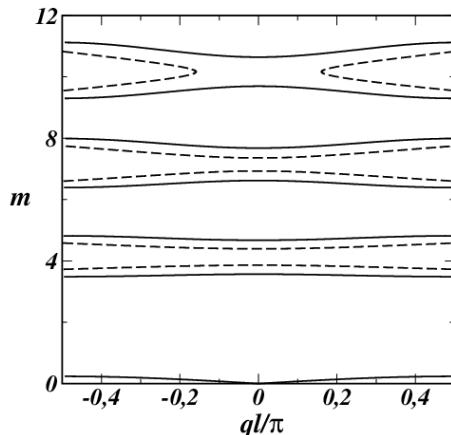
(a) The lowest mass mode for the gravitational field with our dispersion relation (42).



(b) The lowest mass mode for the gravitational field using (13).

Figure 2: The lowest mass modes for the gravitational field with both dispersion relation.

To plot the graphs above we used the definitions (43) and (44). We also made $x = m(l + L)$, and with the relation $l/L = 100$ we obtain $\frac{x}{101} = mL$. We then call $f(x) = (42)^2$, and plotted for $ql = 0.5\pi$ between the upper and lower limit of the cosine. The point where the graph intercepts the x axis for the first time, represents the value of the first mass mode. According to Figure2a), the first mode is at $x = 0.028$ i.e $m = 0.028/(l + L)$, while Figure2b) shows that the first mass mode for (13) is $x = 4$, or $m = 4/(l + L)$. That way our first mode is two order of magnitude smaller than the first mode found in [29]. This leads, as we will see, to a bigger correction in the Newton's law. The comparative between the two dispersion relations, for the first mass modes, is showed in the figure bellow. In this figure, as well as in all the other like this, the y axis represents the mass in units of inverse of length, precisely; $m = x/(l + L)$ or $m = x.(10^{10}mm^{-1})$ once that $l = 10^{-4}mm$ and $L = 10^{-6}mm$.



(a) The lowest mass modes for the gravitational field.

Figure 3: The comparative of the mass modes for the two dispersion relation. The solid curve is our relation, while the dashed curved is the dispersion calculated by [29].

As one can see in Figure 3, the old dispersion relation (dashed curve) says that the lowest mass mode has a maximum in $q \approx 0$. However, within our results, the lowest mode has a minimum in $q \approx 0$. It is also clear the big difference in the values of the first modes. In addition, with the old relation, there is no mass around $q = 0$ for m bigger than $m \approx 9.5$. That is not true according to our relation. Once that we have found the value for the first mass mode, it is possible to estimate the correction in Newton's law due to Bulk gravitons. Here, following a different way as used in [29], we will calculate the correction just due to the first mode. In [29], the author integrated from m_{gap} to infinity. We do not agree with that, once that the mass modes are not continuous (there is a gap between the mass modes). As said in the introduction, the correct expression for the correction to the Newton's Law is given by

$$V \approx -G \frac{m_1 m_2}{r} + \sum_i \int_{m_i}^{M_i} \frac{dm}{K} \frac{G m_1 m_2}{r} \frac{m}{K} e^{-mr}, \quad (45)$$

where $[m_i, M_i]$ are the intervals of allowed mass. Our integral will be calculated from zero because the minimum of mass is at $m = 0$, until the value of $x = 0.028$, that is the maximum for our first mode. To calculate the correction in Newton's law we need the potential of interaction between two particles of mass m_1 and m_2 separated by a distance r , i.e

$$V \approx -G \frac{m_1 m_2}{r} + \left(\int_0^{\frac{0.028}{(i+L)}} \frac{dm}{K} \frac{G m_1 m_2}{r} \frac{m}{K} e^{-mr} \right). \quad (46)$$

After integration we get

$$V \approx -G \frac{m_1 m_2}{r} \left(1 + \frac{0.028 L^2}{(l+L)r^2} e^{\frac{-0.028r}{(l+L)}} \right). \quad (47)$$

The correction found by [29] was

$$V \approx -G \frac{m_1 m_2}{r} \left(1 + \frac{L^2}{(l+L)r} e^{\frac{-4r}{(l+L)}} \right). \quad (48)$$

Taking $r = 1mm$ (the limit where gravity is well tested) as well as the values: $l = 10^{-4}mm$ and $L = 10^{-6}mm$, we have the magnitude of correction, in our case, as $e^{-2.8 \times 10^8}$. While the correction for the old result is $e^{-4 \times 10^{10}}$. It is very clear that our correction is bigger than the previous result.

4 The General setup

In the previous section we developed the specific case of the gravitational field. Now, we will construct the general Schrödinger equation and the dispersion relation that is valid for any bosonic field. In the mathematical process of separation of variables of the equations of motion, we eventually arrive at one point where we deal with an equation of the form [28]

$$\left[-\frac{d^2}{dy^2} + P'(y) \frac{d}{dy} + V(y) \right] \psi(y) = m^2 Q(y) \psi(y). \quad (49)$$

The terms in this equation are $P(y) = \gamma A(y)$, $Q(y) = e^{-2bA(y)}$ and $V(y) = 0$ for all the fields, except for gravity. The equation (49) can be put in the form of a Schrödinger like equation through the transformations

$$\frac{dz}{dy} = f(y), \quad \psi(y) = \Theta(y) \bar{\psi}(z), \quad (50)$$

with

$$f(y) = \sqrt{Q(y)}, \quad \Theta(y) = \exp(P(y)/2) Q(y)^{-1/4}, \quad (51)$$

and

$$\bar{U}(z) = \frac{V(y)}{f^2} + (P'(y)\Omega'(y) - \Omega''(y))/\Omega f^2. \quad (52)$$

In the equations above, the prime symbol is the derivative with respect to y . The expression above is useful when $\frac{dz}{dy} = f(y)$ is not known. When this expression is known, it is better to work with an expression that uses the derivatives in the z coordinate

$$\bar{U}(z) = \bar{V}(z)/\bar{f}^2(z) + \frac{\bar{P}'(z)\bar{\Theta}'(z) - \bar{\Theta}''(z)}{\bar{\Theta}(z)} - \frac{\bar{\Theta}'(z)\bar{f}'(z)}{\bar{\Theta}(z)\bar{f}(z)}, \quad (53)$$

where $f(y) = \bar{f}(z)$. When all these steps are made, we get the desired Schrödinger like equation

$$\left[-\frac{d^2}{dz^2} + \bar{U}(z) \right] \bar{\psi}(z) = m^2 \bar{\psi}(z), \quad (54)$$

with $\bar{U}(z)$ given by

$$\bar{U}(z) = c\bar{A}''(z) + c^2[\bar{A}']^2. \quad (55)$$

As we have $\bar{A}(z) = \ln \Omega(z)/b$, we get

$$\bar{U}(z) = \left(\frac{c}{b} + \frac{c^2}{b^2} \right) \frac{(\Omega^{-1})'^2}{(\Omega^{-1})^2} - \frac{c}{b} \frac{(\Omega^{-1})''}{(\Omega^{-1})}. \quad (56)$$

It is valid to mention that we have used Ω^{-1} in the potential because of its form (6). Now, using the explicit form of Ω^{-1} for $n = 1$, we get the following Schrödinger like equation

$$\Psi'' + \left[m^2 - \left(\frac{c}{b} + \frac{c^2}{b^2} \right) \frac{1}{(S(z) + L)^2} + \frac{2c}{b} \frac{\sum_j (-1)^j \delta(z - jl)}{(S(z) + L)} \right] \Psi = 0. \quad (57)$$

Realize that this equation is very similar to (12), the difference is just some parameters. As these parameters are constants, the procedure to solve this equation for two adjacent cells is identical to the one did in section three. Following exactly the same steps took in the previous section, we arrive at the general dispersion relation

$$\cos(ql) = \frac{\sqrt{-\hat{n}_\nu \hat{n}_{\nu-1} j_\nu j_{\nu-1} - \hat{j}_\nu \hat{j}_{\nu-1} n_\nu n_{\nu-1} + \hat{n}_\nu \hat{j}_{\nu-1} n_\nu j_{\nu-1} + \hat{j}_\nu \hat{n}_{\nu-1} j_\nu n_{\nu-1}}}{(\hat{n}_\nu \hat{j}_{\nu-1} - \hat{j}_\nu \hat{n}_{\nu-1})(n_\nu j_{\nu-1} - j_\nu n_{\nu-1})}. \quad (58)$$

Where $\nu = \left(\frac{1}{2} + \frac{c}{b} \right)$. Then, for each field, with or without the dilaton, we need to find c and b .

5 Revisiting the Bosonic Fields in The Crystal Manifold

Here we will discuss each field separately. We will analyze the fields with and without the dilaton coupling, just like in [35]. We also make some comments about their localization. However, the main goal is to find the parameters that will be used in the dispersion relation.

5.1 The Gravitational Field

As we already discuss the free case, here we will just show how is the behavior of the gravity in the presence of the dilaton, just like in [5, 26]. Again we consider the Einstein's equations in the axial gauge, and the equation that depends on the extra dimension is

$$\left[-e^{2(A-B)} \frac{\partial^2}{\partial y^2} + e^{2(A-B)} B' \frac{d}{dy} + 2e^{2(A-B)} (A'' - A'B' + 2(A')^2) - \partial^2 \right] h_{\mu\nu} = 0, \quad (59)$$

with $\partial^2 \equiv \eta^{\mu\nu} \partial_\mu \partial_\nu$. After the separation of variables $h_{\mu\nu} = \bar{h}_{\mu\nu} \psi(y)$ we get

$$-\psi(y)'' + B' \psi(y)' + 2(A - A'B' + 2(A')^2) \psi(y) = m^2 e^2 (B - A) \psi(y). \quad (60)$$

Using the process described in section four, we get the Schrödinger equation

$$\left(-\frac{d^2}{dz^2} + \bar{U} \right) \bar{\psi} = m^2 \bar{\psi}, \quad (61)$$

with potential

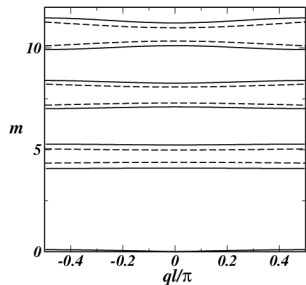
$$\bar{U} = \frac{3}{2} e^{\frac{3}{2}A} \left(A'' + \frac{9}{4} (A')^2 \right). \quad (62)$$

Taking the transformation $\frac{dz}{dy} = e^{-\frac{3}{4}A(y)}$, the potential above gets the form

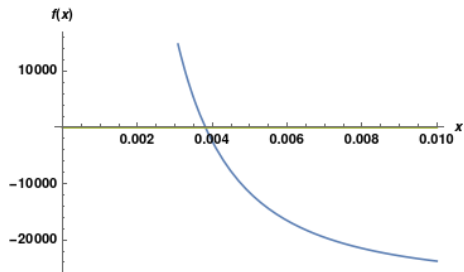
$$\bar{U} = \frac{3}{2} \bar{A}'' + \frac{9}{4} \bar{A}'^2 \quad (63)$$

which is in the form of (55), with $c = \frac{3}{2}$ and, due to the presence of the dilaton, $b = \frac{3}{4}$. In that way, we get the following value for ν : $\nu = \frac{5}{2}$. The localization using the dilaton coupling has been well discussed in [5].

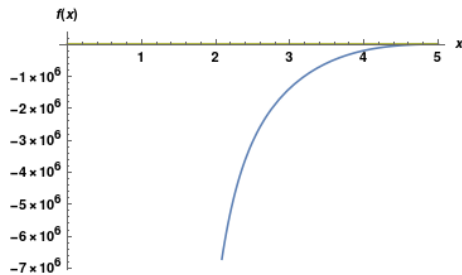
The results for the gravitational field coupled with the dilaton are shown in the figure bellow. Here we have considered the dilaton coupling as $\lambda = 1/\sqrt{(3M^3)}$. We can see that there is a shift in the values of mass, when compared with the results found with the dispersion relation found in [29]. Also, due to the presence of the dilaton, the first mass mode decreases from $m = 0.028/(l+L)$ to $m = 0.004/(l+L)$, in our case. While for the other dispersion, the first mass mode increases from $m_{gap} = 4/(l+L)$ to $m_{gap} = 4.4/(l+L)$.



(a) The lowest mass modes for the gravitational field with the dilaton.



(b) The first mass mode using (42).



(c) The first mass mode using (13).

Figure 4: The lowest mass modes for the gravitational field with the dilaton are represented in (a). The dashed curve is the plot with the wrong dispersion relation, and the solid curve the plot with the correct one. In (b), we have the value for the first mass mode using our relation. In (c), we show the first mass mode for the dispersion relation (13).

5.2 The Scalar Field

Now, we turn our attention to the scalar field in the crystal manifold. Here we will follow the process that was done in [35]. We start with the dilaton free case in which the action is given by

$$S = \frac{1}{2} \int d^5x \sqrt{-g} g^{MN} \partial_M \Phi \partial_N \Phi. \quad (64)$$

The equation of motion obtained is

$$\partial_M [\sqrt{-g} g^{MN} \partial_N \Phi] = 0. \quad (65)$$

The zero mode solution is of the form $\Phi = C\phi(x)$, with C being a constant. This implies an effective action given by

$$S = \int dz \Omega(z)^3 \int d^4x \eta^{\mu\nu} \partial_\mu \phi \partial_\nu \phi. \quad (66)$$

The first integral in the action above is finite. Then the scalar field can be localized in any cell of the crystal. We see that the scalar field does not need any coupling in order to be localized. Yet, in [35], they analyze the case with the dilaton coupling.

Before turning to the case with dilaton, let us first comment the massive modes in the free case. From equation (65), we can get

$$-\phi(y)'' - 4A'(y)\phi(y)' = m^2\phi(y)e^{-2A(y)}, \quad (67)$$

and using the process already described, we have the following potential for the Schrödinger like equation

$$U = e^{2A} \left[\frac{15}{4}A'^2 + \frac{3}{2}A'' \right]. \quad (68)$$

Using the transformation $\frac{dz}{dy} = e^{-A(y)}$ we get

$$\bar{U}(z) = \frac{9}{4}\bar{A}'^2 + \frac{3}{2}\bar{A}''. \quad (69)$$

Then, for the dilaton free case, the scalar field has the same results of the gravitational field with $c = \frac{3}{2}$, and $\nu = 2$. The band structure is the same of Figure 3.

When considering the coupling with the dilaton, the action is of the form

$$S = \int d^5x \sqrt{-g} e^{-\lambda\pi} g^{MN} \partial_M \Phi \partial_N \Phi, \quad (70)$$

where π is the dilaton, and λ is the coupling parameter. The equation of motion, that depends on the extra dimension and that we get from (70), is

$$\phi(y)'' - A' \left(\frac{15}{4} + \lambda\sqrt{3M^3} \right) \phi(y)' = m^2\phi(y)e^{-\frac{3}{2}A}. \quad (71)$$

The Schrödinger equation that we get has as potential

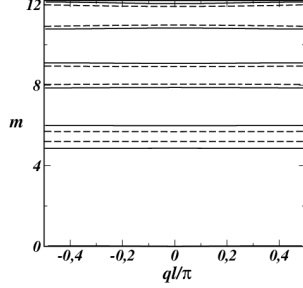
$$U(y) = e^{\frac{3}{2}A} \left[A'^2 \left(\frac{\alpha^2}{4} - \frac{9}{64} \right) - A'' \left(\frac{\alpha}{2} + \frac{3}{8} \right) \right], \quad (72)$$

where $\alpha = -\frac{15}{4} - \lambda\sqrt{3M^3}$. After the change for the z coordinate, with transformation $\frac{dz}{dy} = e^{-\frac{3}{4}A}$, we arrive at

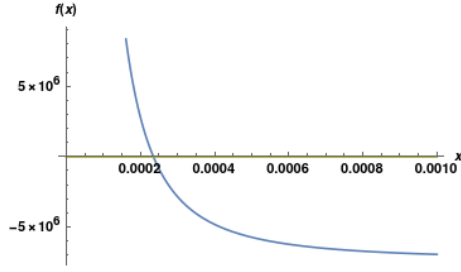
$$\bar{U}(z) = \left[- \left(\frac{\alpha}{2} + \frac{3}{8} \right) A'' + A'^2 \left(\frac{\alpha}{2} + \frac{3}{8} \right)^2 \right]. \quad (73)$$

We then see that $c = \left(\frac{3}{2} + \frac{\lambda\sqrt{3M^3}}{2} \right)$, and $\nu = \left(\frac{5}{2} + 2\lambda\frac{\sqrt{3M^3}}{3} \right)$. As $\lambda = 1/\sqrt{(3M)^3}$, $\nu = 3.17$. Again, the dilaton field decreases the mass for the first mass mode, now the first mass mode is $m = 0.00025/(l + L)$ as can be seen in Figure 5(b).

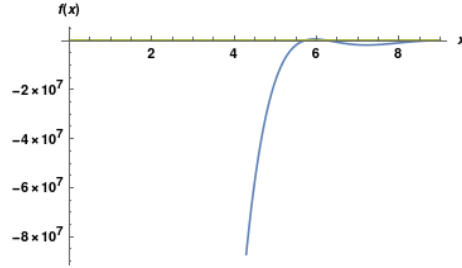
Let us see the band gap structure in this case. Once more the comparison between the two dispersion relation can be seen in Figure 5(a). In Figure 5(b), we have the first mass mode for (42). In Figure 5(c), the first mass mode for (13).



(a) The lowest mass modes for the scalar field with the dilaton.



(b) The first mass mode for our relation.



(c) The first mass mode for (13) .

Figure 5: The lowest mass modes for the scalar field with the dilaton are represented in (a). The dashed curve is the plot with the wrong dispersion relation, and the solid curve the plot with the correct one. In (b), we have the first mode for our relation. In c), the first mode for the old relation.

5.3 The Gauge Field

Let us now see how is the behavior of the gauge field inside the crystal. We will initially consider the free case and, after this, the case with the dilaton coupling. The results about localization will end up being very similar to the cases of just one brane [26, 35]. Again we follow the steps made in [35]. The action for the free case is given by

$$S = -\frac{1}{4} \int d^5 x \sqrt{-g} F_{MN} F^{MN}, \quad (74)$$

with $F_{MN} = \partial_{[M} A_{N]}$ being the field strength of the 1-form field A_M . The equation of motion from action (74) is

$$\partial_M (\sqrt{-g} g^{MP} g^{NQ} F_{PQ}) = 0. \quad (75)$$

From the equation above we get

$$-f(y)'' - 2A'f(y)' = m^2 f e^{-2A}, \quad (76)$$

where we have used the gauge $A_5 = \partial^\mu A_\mu = 0$. With this, the acceptable solution for the zero mode is $f = C$, where C is a constant. Then the gauge field gets the form $A_M = CA_M(x)$, which leads to the effective action

$$S = -\frac{1}{4} \int \Omega(z) dz \int d^4x F_{\mu\nu} F^{\mu\nu}. \quad (77)$$

From the form of $\Omega(z)$, we see that the gauge field is not localized in any cell of the crystal. Some additional term needs to be added in the action in order to achieve localization. The term that will be used by us, just like in [5], is the dilaton one. But, before it, we analyze the massive modes without this case.

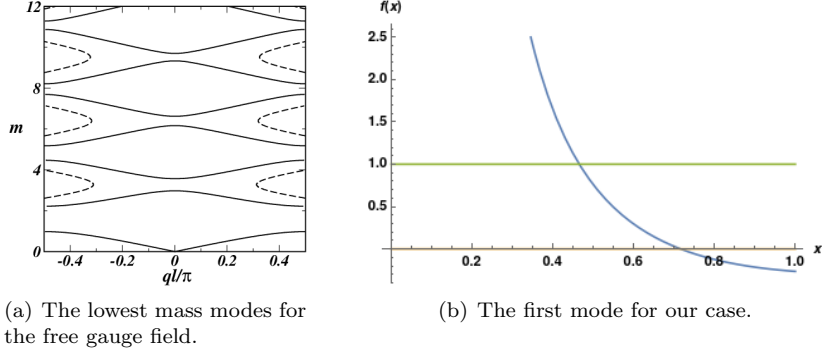
Using the equation (76), and the known process to obtain a Schrödinger like equation, we have the following potential

$$U(y) = e^{2A} \left(\frac{3}{4} A'^2 + \frac{A''}{2} \right), \quad (78)$$

and performing the transformation $\frac{dz}{dy} = e^{-A(y)}$, we get

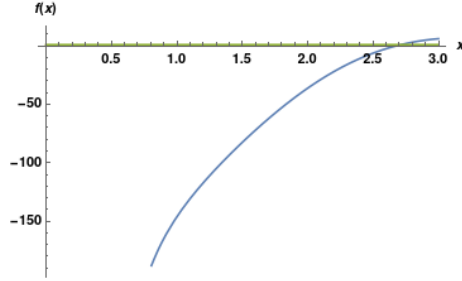
$$\bar{U}(z) = \left[\frac{1}{4} \bar{A}'(z)^2 + \frac{\bar{A}''(z)}{2} \right]. \quad (79)$$

Then we see that in this case $c = \frac{1}{2}$ and $\nu = 1$. Plugging this value in the dispersion relation we get the results showed in the figure bellow. As one can see, differently of what happen in [35], there is mass around $q = 0$. In [35], the mass modes were restricted to $q \approx 0.5\pi/l$, and this is not true. Also from Figure6(b), we see that the first mass mode is $m = 0.7/(l + L)$. In Figure6(c), we plot the first mode for the old result, which the first mode is $m = 2.7/(l + L)$. We can see that our first mode, again, is smaller, leading to a bigger correction in the Coulomb's law.



(a) The lowest mass modes for the free gauge field.

(b) The first mode for our case.



(c) The first mode for [29].

Figure 6: The lowest mass modes for the free gauge field are represented in (a). The dashed curve is the plot with the wrong dispersion relation, and the solid curve the plot with the correct one. b) shows the first mass mode with the correct dispersion. c) The first mode for the wrong dispersion.

When we add the dilaton coupling the action reads

$$S = -\frac{1}{4} \int d^5x \sqrt{-g} e^{-\lambda\pi} F_{MN} F^{MN}. \quad (80)$$

The equation of motion is very similar to (75), but with the difference that the term $e^{-\lambda\pi}$ appear inside the parenthesis. By using the same gauge as before, and the relation $B = \frac{A}{4}$, we achieve

$$-f''(y) - A' \left(\frac{7}{4} + \lambda\sqrt{3M^3} \right) f'(y) = m^2 f(y) e^{-\frac{3}{2}A}. \quad (81)$$

From this equation, and using $\frac{dz}{dy} = e^{-\frac{3}{4}A}$, we get

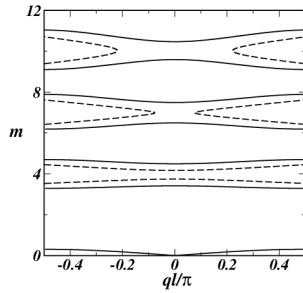
$$\bar{U}(z) = \left[-\bar{A}'' \left(\frac{\alpha}{2} + \frac{3}{8} \right) + \bar{A}'^2 \left(\frac{\alpha}{2} + \frac{3}{8} \right)^2 \right], \quad (82)$$

where $\alpha = -\left(\frac{7}{4} + \lambda\sqrt{3M^3} \right)$, $c = \left(\frac{1}{2} + \frac{\lambda\sqrt{3M^3}}{2} \right)$, which leads to $\nu = \left(\frac{7}{6} + \frac{2\lambda\sqrt{3M^3}}{3} \right)$.

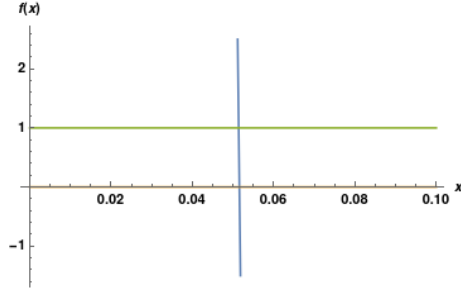
The effective action is

$$S = -\frac{1}{4} \int dy e^{A(\frac{1}{4} + \lambda\sqrt{3M^3})} \int d^4x F_{\mu\nu} F^{\mu\nu}. \quad (83)$$

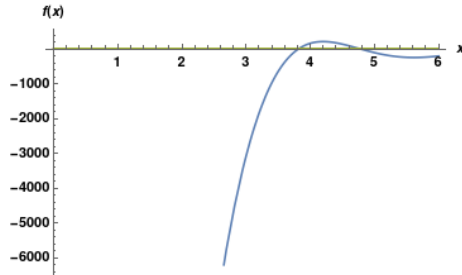
Then, in order to have a gauge field localized in the crystal, we need that $\lambda > -1/4\sqrt{3M^3}$. This is the same condition obtained in the cases with just one brane. Using the same value for the coupling as before, we get $\nu = 1.84$. The band gap structure is showed in the figure below. It is obvious the difference among the solid and dashed curves. For instance, the dashed one tell us that the lowest mode has a maximum in $q = 0$, while the solid says that the lowest mode has a minimum in this value of q . By one hand, for the dashed curve, there is no mass mode allowed around $q = 0$ for $M > 6$. On the other hand, for the correct dispersion relation, there is mass modes around $q = 0$ for $M > 6$. Figure 7(b), tells the value of the first mode: $m = 0.05/(l + L)$. In c), we have the value for the first mode with the wrong dispersion $m = 3.8/(l + L)$.



(a) The lowest mass modes for the gauge field with the dilaton.



(b) The first mass mode with our relation.



(c) The first mass mode for relation (13).

Figure 7: The lowest mass modes for the gauge field with the dilaton are represented in (a). The dashed curve is the plot with the wrong dispersion relation, and the solid curve the plot with the correct one. In (b), we have our first mode. In c) the mode found with dispersion (13).

5.4 The Kalb-Ramond Field

In this subsection we will verify the characteristics of the Kalb-Ramond field in the crystal manifold. This is a rank two anti-symmetric field that appear as a super gravity massless mode in string theory. Here we will follow the same procedure used in [35]. The action for such a field is given by

$$S = -\frac{1}{12} \int d^5x \sqrt{-g} F_{MNR} F^{MNR}, \quad (84)$$

where $F_{MNR} = \partial_{[M} A_{NR]}$ is the field strength for the 2-form field. The equation of motion is

$$\partial_M [\sqrt{-g} g^{ML} g^{NT} g^{RP} F_{LTP}] = 0. \quad (85)$$

From this equation we obtain

$$-f''(y) = m^2 f(y) e^{-2A}. \quad (86)$$

For the zero mode, we have a solution for the field as $A_{MN} = C A_{MN}(x)$. With this and using the gauge $A_{\mu 5} = \partial^\mu A_{\mu\nu} = 0$, we get the effective action

$$S = -\frac{1}{12} \int \Omega(z)^{-2} dz \int d^4x F_{\mu\nu\rho} F^{\mu\nu\rho}. \quad (87)$$

The conclusion is, as $\int \Omega^{-2} dz = \infty$, the two form field is also not localized freely.

The massive modes are studied from equation (86), i.e., we use it to obtain the Schrödinger like equation with potential

$$U(y) = -e^{2A} \left(\frac{A''}{2} + \frac{A'^2}{4} \right). \quad (88)$$

Using the transformation $\frac{dz}{dy} = e^{-A(y)}$, we have

$$\bar{U} = \left(\frac{\bar{A}'^2}{4} - \frac{\bar{A}''}{2} \right). \quad (89)$$

From this we see that $c = -\frac{1}{2}$, and consequently $\nu = 0$. As $\nu = 0$, and remembering the properties of the Bessel functions $j_{-1} = -j_1$ and $n_{-1} = -n_1$, the dispersion relation will be the same that for the case of the free gauge field. These results are showed in Figure6.

If we consider the coupling with the dilaton, the action reads

$$S = -\frac{1}{12} \int d^5x \sqrt{-g} e^{-\lambda\pi} F_{MNR} F^{MNR}. \quad (90)$$

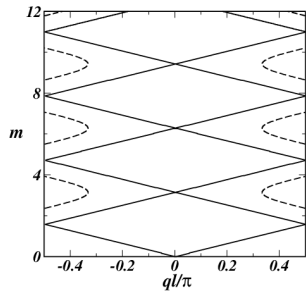
Again, the equation of motion differ from (85) just by the term $e^{-\lambda\pi}$, that will be inside the brackets. However, with this change the analogue equation to (86) is

$$-f(y)'' - f(y)' A' \left(-\frac{1}{4} + \lambda\sqrt{3M^3} \right) = m^2 e^{-\frac{3}{2}A} f(y). \quad (91)$$

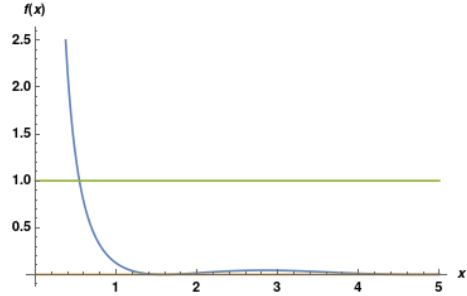
Using the process that we already know, we arrive at one potential identical to (82), but with $\alpha = \frac{1}{4} - \lambda\sqrt{3M^3}$. This leads to $c = -\frac{1}{2} + \frac{\lambda\sqrt{3M^3}}{2}$, and $\nu = -\frac{1}{6} + \frac{2\lambda\sqrt{3M^3}}{3}$, with $\lambda = 1/\sqrt{3M^3}$, $\nu = 0.5$. The effective action in this case is

$$S = -\frac{1}{12} \int dy e^{A(-\frac{7}{4} + \lambda\sqrt{3M^3})} F_{\mu\nu\rho} F^{\mu\nu\rho}. \quad (92)$$

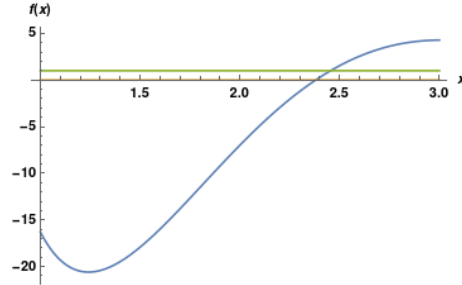
This inform us that the Kalb-Ramond field is localized if $\lambda > 7/4\sqrt{3M^3}$. This case shows an interesting result as we can see in Figure8(a). According to the new dispersion relation, the dispersion for this field (with the dilaton coupling) is linear, at the least for the values of q showed in Figure8(a), i.e., there is no gap between the mass bands. This characteristic does not appear with the wrong dispersion relation used in the work [35]. In b), we see that the value for the first mode in our case is $m = 1.4/(l + L)$. In c), we have the first mode for the wrong dispersion; $m = 2.4/(l + L)$.



(a) The lowest mass modes for the Kalb-Ramond field with the dilaton.



(b) The first mass mode in our case.



(c) The first mass mode with the wrong relation

Figure 8: The lowest mass modes for the Kalb-Ramond field with the dilaton are represented in (a). The dashed curve is the plot with the wrong dispersion relation, and the solid curve the plot with the correct one. In (b), the first mode in our case. In (c), the first mode for the dispersion found in [29].

5.5 The q-Form Field

We are now ready to generalize the cases discussed before, by studying the q-form field in a p-brane in a D-dimensional space, with $p = D - 2$. It was also studied in [35,52], and we follow very like these works. The action for the q-form is

$$S = -\frac{1}{2(q+1)!} \int d^D x \sqrt{-g} F_{M_1 \dots M_{q+1}} F^{M_1 \dots M_{q+1}}, \quad (93)$$

where the general field strength associated to the q-form is $F_{M_1 \dots M_{q+1}} = (q+1)\partial_{[M_1} A_{M_2 \dots M_q]}$. The equation of motion is

$$\partial_{M_1} [\sqrt{-g} F^{M_1 \dots M_{q+1}}] = 0. \quad (94)$$

By doing the process where the equation that depends on the extra dimension is separated from the one that depends on the x^μ , using the gauge $A_{\mu_1 \dots \mu_{q-1} 5} = \partial^{\mu_1} A_{\mu_1 \dots \mu_q} = 0$, and considering the q-form as $A_{M_1 \dots M_q} = A_{M_1 \dots M_q}(x)$, we get

$$-f''(y) - A'(p-2q+1)f' = m^2 e^{-2A} f(y). \quad (95)$$

From the considerations above we get also the effective action

$$S = -\frac{1}{2(p+1)!} \int dy e^{(D-2q-3)A} \int d^{D-1} x F_{\mu_1 \dots \mu_{q+1}} F^{\mu_1 \dots \mu_{q+1}}, \quad (96)$$

that tells us that, in order to obtain a localized q-form, it has to obey the relation $q < \frac{D-3}{2}$. For $D = 5$, we have $q < 1$, showing that in the free case, just the 0-form is localized.

The study of the massive modes is done with the use of equation (95). From this, we get a Schrödinger like equation with potential

$$U(y) = e^{2A} \left[-\bar{A}'^2 \left(q - \frac{p}{2} \right) (p-2q+1) - \bar{A}'' \left(q - \frac{p}{2} \right) - \bar{A}'^2 \left(q - \frac{p}{2} \right) \right]. \quad (97)$$

Through the relation between the coordinates z and y we obtain the potential in the form (55)

$$\bar{U} = \left[\bar{A}'^2 \left(\frac{p}{2} - q \right)^2 + \bar{A}'' \left(\frac{p}{2} - q \right) \right]. \quad (98)$$

Then, we can easily see that $c = \frac{p}{2} - q$, and $\nu = \left(\frac{p+1}{2} - q \right)$. We can now turn our attention to the q-form with the dilaton.

When we consider the action with the dilaton, it takes the form

$$S = -\frac{1}{2(p+1)!} \int d^D x \sqrt{-g} e^{-\lambda\pi} F_{M_1 \dots M_{q+1}} F^{M_1 \dots M_{q+1}}. \quad (99)$$

Using the gauge already mentioned in this subsection, we have the effective action in the form

$$S = -\frac{1}{2(p+1)!} \int dy e^{A(p-2q-3/4+\lambda\sqrt{3M^3})} \int d^{D-1} x F_{\mu_1 \dots \mu_{q+1}} F^{\mu_1 \dots \mu_{q+1}}. \quad (100)$$

As we can see, the localization of the q-form, coupled with the dilaton, obeys the relation $\lambda > \frac{8q-4p+3}{4\sqrt{3M^3}}$.

The equation of motion that we get from action (99) is

$$\partial_{M_1}[\sqrt{-g}e^{-\lambda\pi}F^{M_1\dots M_{q+1}}] = 0. \quad (101)$$

And from this one we have

$$-f''(y) - A'(p - 2q + \lambda\sqrt{3M^3} + 3/4)f'(y) = f(y)m^2e^{-3/2A}. \quad (102)$$

As we already know, from the last formula we have a Schrödinger like equation and, in this case, the potential is

$$\bar{U} = \left[\bar{A}'^2 \left(\frac{\alpha}{2} - \frac{3}{8} \right)^2 + \bar{A}'' \left(\frac{\alpha}{2} - \frac{3}{8} \right) \right]. \quad (103)$$

In the formula above, $\alpha = \frac{4p-8q+3}{4} + \lambda\sqrt{3M^3}$, $c = \frac{\alpha}{2} - \frac{3}{8}$ and $\nu = \frac{2\alpha}{3}$. We can summarize the results of this section in two tables, one for the free case and other for the coupling with the dilaton.

Table 1: Parameters for the cases without dilaton

Field	value of ν	Parameter b	Parameter c
Gravitational	2	1	3/2
scalar	2	1	3/2
Gauge	1	1	1/2
Kalb-Ramond	0	1	-1/2
q-form	$\frac{1+p}{2} - q$	1	$\frac{p}{2} - q$

Table 2: Parameters for the cases with dilaton

Field	value of ν	Parameter b	parameter c
Gravitational	5/2	3/4	3/2
scalar	$\frac{5}{2} + \frac{2\lambda\sqrt{3M^3}}{3}$	3/4	$3/2 + \frac{\lambda\sqrt{3M^3}}{2}$
Gauge	$\frac{7}{6} + \frac{2\lambda\sqrt{3M^3}}{3}$	3/4	$1/2 + \frac{\lambda\sqrt{3M^3}}{2}$
Kalb-Ramond	$-\frac{1}{6} + \frac{2\lambda\sqrt{3M^3}}{3}$	3/4	$-1/2 + \frac{\lambda\sqrt{3M^3}}{2}$
q-form	$\frac{2\alpha}{3}$	3/4	$-\left(\frac{\alpha}{2} + 3/8\right)$

We can also discuss some results for the q-form field. In Figure9(a), according to the dashed curve there are two different regimens, one for $\nu > 1$, and other for $\nu < 1$. For $\nu > 1$ the mass values increases, while for $\nu < 1$ the mass show a parabolic behavior. This is almost what happens with the solid curve, except for the first two values of mass. Part 2) of Figure9(a) shows that the second mass mode tends to zero. Things are completely different in Figure9(b). According to the dashed curve, there is no mass below $\nu \approx 1.6$. And as we

can see, it does not happen for the solid curve. In this way, the analyses done in [35] for the q-form field can not be performed. In that work, they say that by controlling the dilaton coupling it is possible to generate or suppress mass modes, and that is not true, once there is mass for all the values of ν .

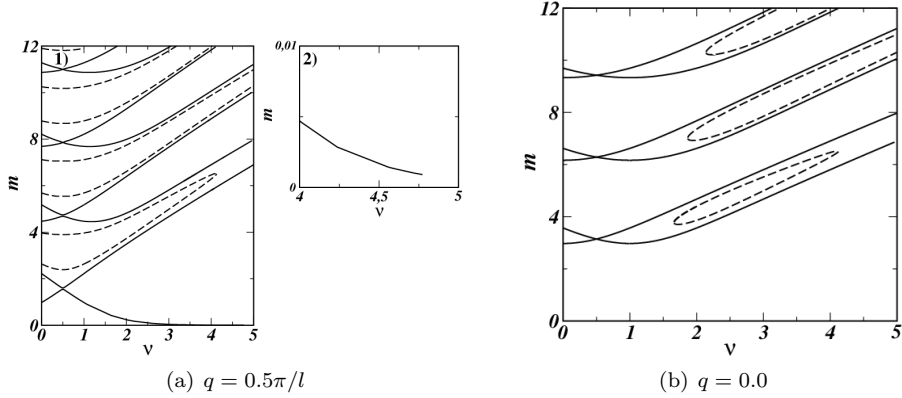


Figure 9: The mass dispersion against the order of the Bessel(Be aware that q in this figure represents the wave vector momentum.)

What is still valid for both dispersion relation is the plot of the mass against the separation between the branes l , as you can see in Figure 10. There, the plot was done for different values of ν . It shows that the mass decreases as $m(l) \propto \frac{1}{l}$. In the limit of $l \rightarrow \infty$ there will be no gap, and the behavior of the system is like that with just one brane [4].

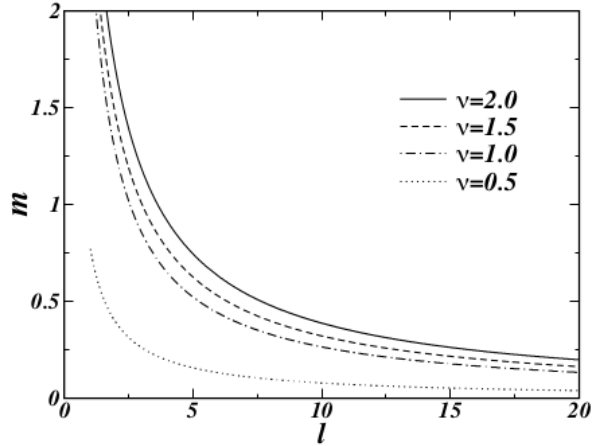


Figure 10: The lowest mass modes against the distance between the branes.

6 Bosonic Fields in the Crystal Manifold (With Non-minimal Coupling)

In this section we will study the gauge, Kalb-Ramond and q-form fields in the background of the crystal manifold. The results of this section are new, and that way there is no comparison to be made. This time we take the couplings with geometrical quantities: the Ricci scalar and the Ricci tensor. The Schrödinger equation will be very like (57), but with the difference that $b = 1$, once that now there is no dilaton coupling. As the Schrödinger equation changes just for a constant, the dispersion relation still remains as in (58). We start with the study of the gauge field. Also, because $b = 1$, the metric is $ds^2 = e^{2A(y)}\eta_{\mu\nu}dx^\mu dx^\nu + dz^2$, and the value of ν is $\nu^2 = (\frac{1}{2} + c_1)^2$.

6.1 The Gauge Field

We start our discussion with both couplings: the Ricci scalar and the Ricci tensor. The action, in five dimensions, takes the form

$$S = - \int d^5x \sqrt{-g} \left[\frac{1}{4} F_{MN} F^{MN} + \frac{\lambda_1}{2} R A_M A^M + \frac{\lambda_2}{2} R_{MN} A^M A^N \right]. \quad (104)$$

Here $F_{MN} = \partial_{[M} A_{N]}$. The equation of motion that we obtain from this action is

$$\partial_M [\sqrt{-g} F^{MN}] = \lambda_1 \sqrt{-g} R A^N + \lambda_2 \sqrt{-g} R^{MN} A_M. \quad (105)$$

Due to the fact that F^{MN} be antisymmetric, we have from the above equation

$$\partial_\mu [\lambda_1 e^{3A} R A^\mu + \lambda_2 e^A R_\nu^\mu A^\nu] = -\partial_5 [\lambda_1 e^{3A} R A^5 + \lambda_2 e^A R_5^\mu A^\mu] = 0. \quad (106)$$

From equation (105), we get the following equations

$$\partial_5 [e^A F^{5\nu}] + \partial_\mu [e^A F^{\mu\nu}] = \lambda_1 e^{3A} R A^\nu + \lambda_2 e^A R_\mu^\nu A^\mu = 0, \quad (107)$$

and

$$\partial_\mu F^{\mu 5} = \lambda_1 e^{2A} R A^5 + \lambda_2 R_5^\mu A^\mu. \quad (108)$$

Now, by using the identities in [10], which are $\partial_\mu F^{\mu\nu} = \square A_T^\nu$; $F^{5\mu} = \partial_5 A_T^\mu + F_L^{5\mu}$; $F_L^{\mu 5} = \frac{\partial^\mu}{\square} \partial_\nu F^{\nu 5}$ and the separation for the field $A^\mu = A_T^\mu + A_L^\mu$, where A_T^μ is the transverse part of the field and A_L^μ is the longitudinal one, we can have from equation (108)

$$\partial_\mu F_L^{\mu 5} - \lambda_1 e^{2A} R A^5 - \lambda_2 R_5^\mu A^\mu = 0. \quad (109)$$

Using the identities in (107), we get

$$\begin{aligned} & e^A \square A_T^\nu + \partial_5 [e^A \partial_5 A_T^\nu] + \partial_5 [e^A F_L^{5\nu}] \\ & - \lambda_1 e^{3A} R A_T^\nu - \lambda_1 e^{3A} R A_L^\nu - \lambda_2 e^A R_\mu^\nu A_T^\mu - \lambda_2 e^A R_\mu^\nu A_L^\mu = 0. \end{aligned} \quad (110)$$

With the help of the mentioned identities, we can prove that

$$\partial_5[e^A F_L^{5\nu}] = \lambda_1 e^{3A} R A_L^\nu + e^A \lambda_2 R_\alpha^\nu \square (\partial_\mu A_L^\mu) = \lambda_1 e^{3A} R A_L^\nu + \lambda_2 e^A R_\mu^\nu A_L^\mu. \quad (111)$$

By replacing (111) in (110), we have

$$e^A \square A_T^\nu + \partial_5[e^A \partial_5 A_T^\nu] - \lambda_2 e^A \frac{R_\beta^\beta}{4} A_T^\nu = 0. \quad (112)$$

In order to solve the above equation, we propose the following ansatz: $A_T^\nu(x, z) = e^{-\frac{A}{2}} \chi(y) \hat{A}_T^\nu(x)$. With that we have for the function of the extra dimension

$$\chi'' - \left[A'' \left(\frac{1}{2} - 8\lambda_1 - \lambda_2 \right) + A'^2 \left(\frac{1}{4} - 12\lambda_1 - 3\lambda_2 \right) \right] \chi = -m^2 \chi. \quad (113)$$

Here we can define $c_1 = \frac{1}{2} - 8\lambda_1 - \lambda_2$ and $c_2 = \frac{1}{4} - 12\lambda_1 - 3\lambda_2$. For the zero mode, the equation above admits a solution of the form $\chi = e^{aA}$. The potential of (113) is of the form $U = c_1 A'' + c_2 A'^2$. Using the solution proposed, it is easy to see that $c_1 = a$ and $c_2 = a^2$, or just $c_1^2 = c_2$. However, just with this condition we can not find the two coupling constants. In order to find both of them we need one more condition. This condition is obtained observing the asymptotic behavior of the potential in (113). In essence we observe the behavior of the warp factor $A(y)$. The general case is well done in [14]. The condition found in [14] was $2c_1 > d$, where d is the number of extra dimensions and, in our case, $d = 1$. We will use these two conditions, $c_1^2 = c_2$ and $2c_1 > 1$, to find the values of λ_1 and λ_2 . Using the condition $c_1^2 = c_2$, we obtain

$$\lambda_2^\pm = -(1 + 8\lambda_1) \pm \sqrt{12\lambda_1 + 1}. \quad (114)$$

Getting λ_2^+ , and using the formula for c_1 , we have $c_1^+ = \frac{3}{2} - \sqrt{12\lambda_1 + 1}$. In the same way, with λ_2^- we have $c_1^- = \frac{3}{2} + \sqrt{12\lambda_1 + 1}$. With c_1^- and the condition $2c_1 > 1$ we get $\lambda_1 \geq -\frac{1}{12}$. With c_1^+ we have $\lambda_1 < 0$. If we get the value $\lambda_1 = -\frac{1}{12}$, and put in λ_2^\pm we obtain $\lambda_2 = -\frac{1}{3}$. Substituting λ_1 and λ_2 in c_1 and c_2 , we get $c_1 = \frac{3}{2}$ and $c_2 = \frac{9}{4}$. This leads to the solution $\chi = e^{\frac{3}{2}A}$ for the zero mode of (113). The effective action for the zero mode is given by

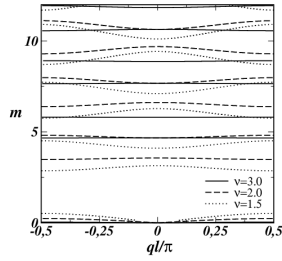
$$S_{eff} = - \int e^{3A(z)} dz \left[\int d^4x \frac{1}{4} \tilde{F}_T^{\mu\nu} \tilde{F}_{\mu\nu}^T \right]. \quad (115)$$

And with $A(z) = -\ln(K|z| + 1)$, we get for the first integral in the above action the value $\frac{1}{k}$. Then we have a zero mode localized in the brane.

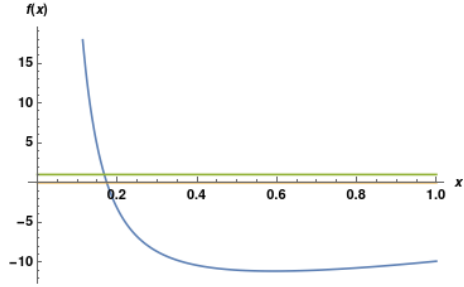
We can now analyze the values of ν that will be used in the dispersion relation (58). The value of ν is $\nu = (\frac{1}{2} + c_1)$. Placing the value of c_1 we find that $\nu = 2$. We realize that this value is the same of the cases of the free scalar and free gravitational fields. However, we can make some changes. For example, we can make $\lambda_1 = 0$ which means to take off the Ricci Scalar, which means that

we are in a model like in [48]. With that, we get $\nu = 3$. We can also turn off the parameter λ_2 , putting the Ricci tensor out of the game, this model is showed in [10]. By doing that, we arrive at $\nu = \frac{3}{2}$. From the equation (108), we see that we have to deal with the localization of a scalar field. But we will not focus in this part.

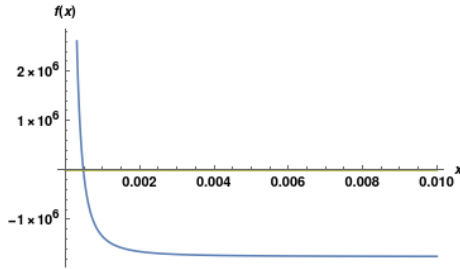
The results for the mass modes that we get in this case are showed in Figure 11. The results for $\nu = 2$ were already showed in Figure 3. In Figure 11, when λ_1 is turned off (there is just the Ricci tensor) we have $\nu = 3$. For $\lambda_2 = 0$, we have $\nu = \frac{3}{2}$. We also realize that there is a big gap between the first mass mode and the next ones. This tell us that just the first mass mode has a chance to be found, in the near future. The value for the first mass mode for $\nu = 1.5$ and $\nu = 3$ are, respectively, $m = 0.16/(l + L)$ and $m = 3.4/(l + L)$. For $\nu = 2$, the first mass mode, as we saw before, is $m = 0.028/(l + L)$. After the conversion we get one mass of order $6.2 \times 10^{-31} \text{ kg}$. This is above the lower bound limit imposed in the tests for a massive photon [53].



(a) Gauge field with both couplings $\nu = 2$, just with the Ricci scalar $\nu = 1.5$ and just with the Ricci tensor $\nu = 3$



(b) The first mass mode for $\nu = 1.5$.



(c) The first mass mode for $\nu = 3$

Figure 11: The allowed mass modes with the geometrical coupling (gauge field), and the first mass modes. In b), the first mass mode for the coupling just with the Ricci scalar. In c), the first mass mode for the coupling just with the Ricci tensor.

6.2 The Kalb-Ramond Field

Let us now turn our attention to the Kalb-Ramond field. While in the localization process of the 1-form field we get a scalar field along the way, in the dimensional reduction of the Kalb-Ramond field we have a 2-form field localized and also a 1-form field. In that way, the localization of the Kalb-Ramond field induces a localization of a 1-form field as discussed in [51]. The action for the Kalb-Ramond field in five dimensions with the two geometric quantities is

$$S = - \int d^5x \sqrt{-g} \left[\frac{1}{12} F_{M_1 M_2 M_3} F^{M_1 M_2 M_3} + \frac{\lambda_1}{4} R A^{M_2 N_2} A_{M_2 N_2} + \frac{\lambda_2}{4} g^{N_1 N_2} R^{M_1 M_2} A_{M_1 N_1} A_{M_2 N_2} \right]. \quad (116)$$

Where $F_{M_1 M_2 M_3} = (q+1)\partial_{[M_1} A_{M_2 M_3]}$, with $q = 2$. This action leads to the following equation of motion

$$\partial_{M_1} [\sqrt{-g} F^{M_1 M_2 M_3}] - \lambda_1 \sqrt{-g} R A^{M_2 M_3} - \lambda_2 \sqrt{-g} g^{N_1 [M_3} R^{M_2] M_1} A_{M_1 N_1} = 0. \quad (117)$$

The last term appears anti-symmetrized due to $A_{M_1 M_2}$ be antisymmetric. Just like we did in the case of the 1-form field, we use the fact that the field strength is completely antisymmetric to get the following equation from (117)

$$\partial_{M_2} [\lambda_1 \sqrt{-g} R A^{M_2 M_3} + \lambda_2 \sqrt{-g} g^{N_1 [M_3} R^{M_2] M_1} A_{M_1 N_1}] = 0. \quad (118)$$

We can split the equation (117) in two parts, one tensorial and other vectorial. By fixing $M_2 = \nu$ and $M_3 = 5$, we get the vector part as

$$\partial_\mu F^{\mu\nu 5} - \lambda_1 e^{2A} R A^{\nu 5} - \frac{\lambda_2}{2} R_5^5 A^{\nu 5} - \frac{\lambda_2}{2} \frac{R_\beta^\beta}{4} A^{\nu 5} = 0. \quad (119)$$

When we fix $M_2 = \mu$ and $M_3 = \nu$ in (117), we have the tensor part given by

$$\partial_\rho F^{\rho\mu\nu} + e^A \partial_5 [e^{-A} F^{5\mu\nu}] - \lambda_1 e^{2A} R A^{\mu\nu} - \lambda_2 \frac{R_\beta^\beta}{4} A^{\mu\nu} = 0. \quad (120)$$

We now work with equation (118). We make $M_3 = 5$ to get

$$\partial_\mu (\lambda_1 e^A R A^{\mu 5}) + (\lambda_2 e^{-A} \frac{R_\beta^\beta}{8} + \frac{\lambda_2}{2} e^{-A} R_5^5) \partial_\mu A^{\mu 5} = 0. \quad (121)$$

From the last equation, we see that the vector field $A^{\mu 5}$, once that R , R_β^β and R_5^5 depends only of $A(y)$ and its derivative, obeys the transverse condition $\partial_\mu A^{\mu 5} = 0$. For $M_3 = \nu$ in (118), we obtain

$$\partial_5 \left[\lambda_1 R e^A + \frac{\lambda_2}{2} e^{-A} \left(R_5^5 + \frac{R_\beta^\beta}{4} \right) \right] A^{5\nu} + \partial_\mu \left[\lambda_1 e^A R + \lambda_2 e^{-A} \frac{R_\beta^\beta}{4} \right] A^{\mu\nu} = 0. \quad (122)$$

We see that the Kalb-Ramond field does not have null divergence. Because of that we split it like done in [50, 51]

$$A_T^{\mu\nu} = A^{\mu\nu} + \frac{1}{\square} \partial^{[\mu} \partial_\rho A^{\nu]\rho} \quad ; \quad A_L^{\mu\nu} = -\frac{1}{\square} \partial^{[\mu} \partial_\rho A^{\nu]\rho}. \quad (123)$$

We have to show that the longitudinal and transverse part of the field can be decoupled. For this we use the identities

$$\partial_\mu F^{\mu\nu\rho} = \square A_T^{\nu\rho} \quad ; \quad F_L^{5\mu\nu} = -\frac{1}{\square} \partial^{[\mu} \partial_\rho F^{\nu]\rho 5} \quad ; \quad F^{\mu\nu 5} = \partial^5 A_T^{\mu\nu} + F_L^{\mu\nu 5}. \quad (124)$$

We now use (124) in (120), the result is

$$\begin{aligned} & \square A_T^{\mu\nu} + e^A \partial_5 [e^{-A} \partial^5 A_T^{\mu\nu}] + e^A \partial_5 [e^{-A} F_L^{5\mu\nu}] \\ & - \lambda_1 e^{2A} R A_T^{\mu\nu} - \lambda_1 e^{2A} R A_L^{\mu\nu} - \lambda_2 \frac{R_\beta^\beta}{4} A_T^{\mu\nu} - \lambda_2 \frac{R_\beta^\beta}{4} A_L^{\mu\nu} = 0 \end{aligned} \quad (125)$$

With the help of the second identity in (124), and with the equation (119) and (122), we show that

$$e^A \partial_5 [e^{-A} F_L^{5\mu\nu}] = \left(\lambda_1 e^{2A} R + \lambda_2 \frac{R_\beta^\beta}{4} \right) A_L^{\mu\nu}. \quad (126)$$

Placing (126) in (125) we arrive at

$$\square A_T^{\mu\nu} + e^A \partial_5 (e^{-A} \partial^5 A_T^{\mu\nu}) - \lambda_1 e^{2A} R A_T^{\mu\nu} - \lambda_2 \frac{R_\beta^\beta}{4} A_T^{\mu\nu} = 0. \quad (127)$$

The standard solution that is proposed to solve the above equation is $A_T^{\mu\nu} = e^{\frac{A}{2}} \tilde{A}_T^{\mu\nu}(x) \psi(z)$. By plugging this solution in (127) we have

$$\psi'' - \left[A'' \left(-\frac{1}{2} - 8\lambda_1 - \lambda_2 \right) + A'^2 \left(\frac{1}{4} - 12\lambda_1 - 3\lambda_2 \right) \right] \psi = -m^2 \psi. \quad (128)$$

Like we did in the previous subsection, we have to use two conditions to determine λ_1 and λ_2 . Here $c_1 = -\frac{1}{2} - 8\lambda_1 - \lambda_2$ and $c_2 = \frac{1}{4} - 12\lambda_1 - 3\lambda_2$. The conditions are the same used in the case of the gauge field. By using them we have

$$\lambda_2^\pm = -8\lambda_1 - 2 \pm 2\sqrt{3\lambda_1 + 1}. \quad (129)$$

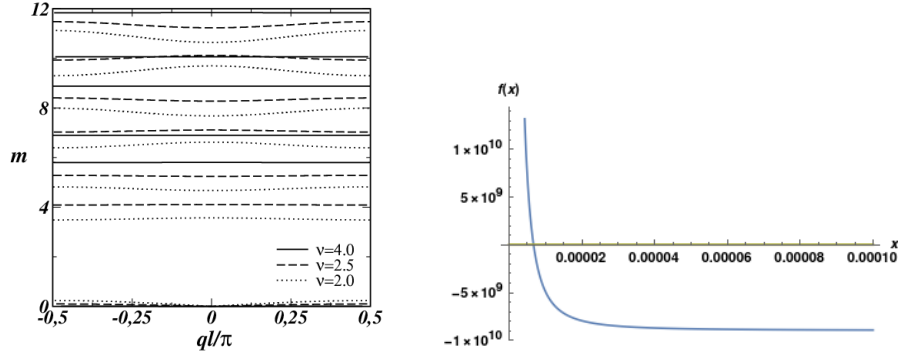
Substituting λ_2^+ in c_1 , we find $\lambda_1 < -\frac{1}{4}$. With λ_2^- we get $\lambda_1 \geq -\frac{1}{3}$. Using $\lambda_1 = -\frac{1}{3}$ in λ_2 , we find $\lambda_2 = \frac{2}{3}$. With the values of λ_1 and λ_2 at hand, we find that $c_1 = \frac{3}{2}$ and $c_2 = \frac{9}{4}$. Coincidentally, we find the same values as for the gauge field. With that, the solution is given by $\psi = e^{\frac{3}{2}A}$.

With $c_1 = \frac{3}{2}$ we have $\nu = 2$. However, if we make $\lambda_2 = 0$, model treated in [51], we have $c_1 = 2$ which leads to $\nu = \frac{5}{2}$. Also, if we turn off the λ_1

parameter, model studied in [49], we get $c_1 = \frac{7}{2}$, then $\nu = 4$. The effective action for the zero mode of the Kalb-Ramond field is

$$S_{eff} = -\frac{1}{12} \int e^{3A} dz \int d^4x \hat{F}_{\mu\nu\rho}^T \hat{F}_T^{\mu\nu\rho}, \quad (130)$$

and this represents the action of a localized zero mode on the brane. The plots for the Kalb-Ramond field are showed in Figure12. When considering both couplings, we have $\nu = 2$. Just like in the case of the gauge field. If we take off the Ricci tensor, we have $\nu = 2.5$. By making $\lambda_1 = 0$ (just the Ricci tensor), we get $\nu = 4$. The first mass mode for $\nu = 2.5$ and $\nu = 4$ are, respectively, $m = 0.004/(l+L)$ and $m = 0.000006/(l+L)$. In the figure bellow, we plot just the first mode for $\nu = 4$, once that for $\nu = 2$ and $\nu = 2.5$ were already plotted in Figures2 and 4.



(a) Kalb-Ramond field with both couplings $\nu = 2$, just with the Ricci scalar $\nu = 2.5$ and just with the Ricci tensor $\nu = 4$

(b) The first mass mode for $\nu = 4$

Figure 12: The allowed mass modes with the geometrical coupling(Kalb-Ramond field). In b), the first mass when the field is coupled just with the Ricci tensor.

6.3 The q-Form Field

Now we generalize the previous results to the case of the q-form field. We will see if it is possible to localize it in a $(D-1)$ -brane, and also analyze the value of ν . The action for the q-form with both couplings is

$$S = - \int d^Dx \sqrt{-g} \left[\frac{1}{2(q+1)!} F_{M_1 M_2 \dots M_{q+1}} F^{M_1 M_2 \dots M_{q+1}} + \frac{\lambda_1}{2q!} R A_{M_2 \dots M_{q+1}} A^{M_2 \dots M_{q+1}} \right. \\ \left. + \frac{\lambda_2}{2q!} g_{M_1 N_1} R^{M_1 M_2} g^{N_1 N_2} g^{M_3 N_3} \dots g^{M_{q+1} N_{q+1}} A_{M_2 M_3 \dots M_{q+1}} A_{N_2 N_3 \dots N_{q+1}} \right]. \quad (131)$$

The field strength is given by $F_{M_1 M_2 \dots M_{q+1}} = (q+1)\partial_{[M_1} A_{M_2 M_3 \dots M_{q+1}]}$. The equation of motion that we obtain from (131) is

$$\begin{aligned} \partial_{M_1} [\sqrt{-g} F^{M_1 M_2 \dots M_{q+1}}] - \lambda_1 R \sqrt{-g} A^{M_2 M_3 \dots M_{q+1}} \\ - \frac{\lambda_2}{2} \sqrt{-g} g_{M_1 N_1} R^{M_1 [M_2} A^{N_1 M_3] \dots M_{q+1}}. \end{aligned} \quad (132)$$

In the equation above the indices M_2 and M_3 are anti-symmetrized. Just like in the previous two cases, we use the anti-symmetry of the field strength to obtain

$$\partial_{M_2} \left[\sqrt{-g} \lambda_1 R A^{M_2 M_3 \dots M_{q+1}} + \frac{\lambda_2}{2} \sqrt{-g} g_{M_1 N_1} R^{M_1 [M_2} A^{N_1 M_3] \dots M_{q+1}} \right] = 0. \quad (133)$$

What we have to do now is decompose the q-form in D-dimensions in a q-form and a (q-1)-form in (D-1)-dimensions. In order to do that we have to expand the equation (132). With this expansion, we will get two different equations, one with one of the free indices equal 5 and other which none of the free indices equal to 5.

By doing $M_2 = 5$ in (132), substituting the $\sqrt{-g}$ and the term of the metric, the equation of motion becomes

$$\begin{aligned} \partial_{\mu_1} [e^{\alpha_q A} F^{\mu_1 \mu_2 \dots \mu_q 5}] - e^{\beta_q A} \lambda_1 R A^{\mu_2 \dots \mu_q 5} \\ - \frac{\lambda_2}{2} e^{\alpha_q A} \left(R_5^5 + \frac{R_\beta^\beta}{4} \right) A^{\mu_2 \dots \mu_q 5} = 0. \end{aligned} \quad (134)$$

Making $M_2 = \mu_2$ in (132), we get

$$\begin{aligned} e^{\alpha_q A} \partial_{\mu_1} F^{\mu_1 \mu_2 \dots \mu_q \mu_{q+1}} + \partial_5 [e^{\alpha_q A} F^{5 \mu_2 \dots \mu_q \mu_{q+1}}] \\ - e^{\beta_q A} \lambda_1 R A^{\mu_2 \mu_3 \dots \mu_q \mu_{q+1}} - \lambda_2 e^{\alpha_q A} \frac{R_\beta^\beta}{4} A^{\mu_2 \dots \mu_q \mu_{q+1}} = 0. \end{aligned} \quad (135)$$

Where $\alpha_q = [D - 2(q+1)]$ and $\beta_q = (D - 2q)$. In the case of the 1-form, we have $\partial_\mu F^{\mu 5} - \lambda_1 R e^{2A} A^5 - \lambda_2 R_5^5 A^5 = 0$, i.e., the equation (134) is not valid for the 1-form. This is due to the fact that none of the indices of $R^{M_1 M_2}$ be anti-symmetrized with the indices of the field. In that way we can correct the equation (134) in the following way

$$\begin{aligned} \partial_{\mu_1} [e^{\alpha_q A} F^{\mu_1 \mu_2 \dots \mu_q 5}] - e^{\beta_q A} \lambda_1 R A^{\mu_2 \mu_3 \dots \mu_q 5} \\ - \lambda_2 e^{\alpha_q A} \frac{(R_5^5 + k R_\beta^\beta)}{(k+1)} A^{\mu_2 \mu_3 \dots \mu_q 5} = 0, \end{aligned} \quad (136)$$

where $k = 0$ for the 1-form and $k = 1$ for the rest. Now, we turn our attention to (133). By making some changes in the indices we can write it as

$$\partial_{M_1} [\sqrt{-g} \lambda_1 R A^{M_1 M_2 \dots M_q}] + \partial_{M_1} \left[\frac{\lambda_2 \sqrt{-g}}{2} g_{N_3 N_1} R^{N_3 [M_1} A^{N_1 M_2] \dots M_q} \right] = 0. \quad (137)$$

Then, fixing $M_2 = 5$ in (137), we get the divergence condition to the (q-1)-form $\partial_{\mu_1} A^{\mu_1 \mu_2 \dots \mu_{q-1} 5} = 0$. Making $M_2 = \mu_2$ in (137), we get

$$\begin{aligned} \partial_5 \left[e^{\beta_q A} R \lambda_1 A^{\mu_1 \dots \mu_{q-1} 5} + e^{\alpha_q A} \frac{(R_5^5 + k R_\beta^\beta)}{(k+1)} A^{\mu_1 \mu_2 \dots \mu_{q-1} 5} \right] \\ + \left[e^{\beta_q A} \lambda_1 R + \lambda_2 e^{\alpha_q A} \frac{R_\beta^\beta}{4} \right] \partial_{\mu_1} A^{\mu_1 \mu_2 \dots \mu_q} = 0. \end{aligned} \quad (138)$$

Then we see that a q-form has no null divergence. Just like in all the previous cases, we propose the decomposition of it in its transverse and longitudinal parts

$$\begin{aligned} A_T^{\mu_1 \mu_2 \dots \mu_q} &= A^{\mu_1 \mu_2 \dots \mu_q} + \frac{(-1)^q}{\square} \partial^{[\mu_1} \partial_{\nu_1} A^{\mu_2 \dots \mu_q] \nu_1} \\ A_L^{\mu_1 \mu_2 \dots \mu_q} &= \frac{(-1)^{q-1}}{\square} \partial^{[\mu_1} \partial_{\nu_1} A^{\mu_2 \dots \mu_q] \nu_1} \\ A^{\mu_1 \mu_2 \dots \mu_q} &= A_T^{\mu_1 \mu_2 \dots \mu_q} + A_L^{\mu_1 \mu_2 \dots \mu_q}. \end{aligned} \quad (139)$$

By using (139) we can write (135) as

$$\begin{aligned} e^{\alpha_q A} \partial_\nu F^{\nu \mu_1 \dots \mu_q} + \partial_5 [e^{\alpha_q A} F^{5 \mu_1 \dots \mu_q}] - e^{\beta_q A} \lambda_1 R A_T^{\mu_1 \dots \mu_q} \\ - e^{\beta_q A} \lambda_1 R A_L^{\mu_1 \dots \mu_q} - \lambda_2 e^{\alpha_q A} \frac{R_\beta^\beta}{4} A_T^{\mu_1 \dots \mu_q} - \lambda_2 e^{\alpha_q A} \frac{R_\beta^\beta}{4} A_L^{\mu_1 \dots \mu_q} = 0. \end{aligned} \quad (140)$$

We yet use the generalized identities for the q-form that can be found at [48,50]

$$\begin{aligned} F^{\mu_1 \mu_2 \dots \mu_q 5} &= F_L^{\mu_1 \mu_2 \dots \mu_q 5} + \partial^5 A_T^{\mu_1 \mu_2 \dots \mu_q} \\ F_L^{\mu_1 \mu_2 \dots \mu_q 5} &= \frac{(-1)^{q-1}}{\square} \partial^{[\mu_1} \partial_\nu F^{\mu_2 \dots \mu_q] \nu 5} \\ \partial_\nu F^{\nu \mu_1 \dots \mu_q} &= \square A_T^{\mu_1 \dots \mu_q}. \end{aligned} \quad (141)$$

Substituting (141) in (140), we get

$$\begin{aligned} e^{\alpha_q A} \square A_T^{\mu_1 \dots \mu_q} + \partial_5 [e^{\alpha_q A} (F_L^{5 \mu_1 \dots \mu_q})] + \partial_5 [e^{\alpha_q A} (\partial^5 A_T^{\mu_1 \dots \mu_q})] \\ - e^{\beta_q A} \lambda_1 R A_T^{\mu_1 \dots \mu_q} - e^{\beta_q A} \lambda_1 R A_L^{\mu_1 \dots \mu_q} - \lambda_2 e^{\alpha_q A} \frac{R_\beta^\beta}{4} A_T^{\mu_1 \dots \mu_q} - \lambda_2 e^{\alpha_q A} \frac{R_\beta^\beta}{4} A_L^{\mu_1 \dots \mu_q} = 0. \end{aligned} \quad (142)$$

By using the second identity in (141),(136),(138) and (139) we can show that the second term in (142) is

$$\partial_5 [e^{\alpha_q A} (F_L^{5 \mu_1 \dots \mu_q})] = \left(e^{\beta_q A} \lambda_1 R + \lambda_2 e^{\alpha_q A} \frac{R_\beta^\beta}{4} \right) A_L^{\mu_1 \dots \mu_q}. \quad (143)$$

Then, plugging (143) in (142) we have

$$\begin{aligned} e^{\alpha_q A} \square A_T^{\mu_1 \dots \mu_q} + \partial_5 [e^{\alpha_q A} (\partial^5 A_T^{\mu_1 \dots \mu_q})] \\ - e^{\beta_q A} \lambda_1 R A_T^{\mu_1 \dots \mu_q} - \lambda_2 e^{\alpha_q A} \frac{R_\beta^\beta}{4} A_T^{\mu_1 \dots \mu_q} = 0. \end{aligned} \quad (144)$$

As a solution for the above equation we propose $A_T^{\mu_1 \dots \mu_q} = \hat{A}_T^{\mu_1 \dots \mu_q}(x) e^{-\frac{\alpha_q A}{2}} \psi(z)$. With this solution in (144) we separate the variables obtaining one equation that depends on the extra dimension and other that has a x^μ dependence. The equation that depends on the extra dimension is

$$\psi'' - \left[A'' \left(\frac{\alpha_q}{2} - 2\lambda_1(D-1) - \lambda_2 \right) + A'^2 \left(\frac{\alpha_q^2}{4} - \lambda_1(D-1)(D-2) - \lambda_2(D-2) \right) \right] \psi = -m^2 \psi \quad (145)$$

where we have used the Ricci scalar and Ricci tensor in D - dimensions computed in [14, 48]. Here we have c_1 and c_2 as $c_1 = \frac{\alpha_q}{2} - 2\lambda_1(D-1) - \lambda_2$, $c_2 = \frac{\alpha_q^2}{4} - \lambda_1(D-1)(D-2) - \lambda_2(D-2)$. In order to determine λ_1 and λ_2 we use the same process as before, using $c_1^2 = c_2$ and $2c_1 > d$, where d is the number of extra dimensions. By using the condition $c_1^2 = c_2$ we get

$$\lambda_2^\pm = -\frac{[-\alpha_q + 4\lambda_1(D-1) + (D-2)]}{2} \pm \frac{1}{2} \sqrt{\alpha_q^2 + 4\lambda_1(D-1)(D-2) - 2\alpha_q(D-2) + (D-2)^2}. \quad (146)$$

We then use the second condition $2c_1 > d$, together with the values of λ_2 , to find the range of values for λ_1

$$\frac{2\alpha_q(D-2) - (D-2)^2 - \alpha_q^2}{4(D-1)(D-2)} \leq \lambda_1 < \frac{(D-d-2)^2 + 2\alpha_q(D-2) - (D-2)^2 - \alpha_q^2}{4(D-1)(D-2)}. \quad (147)$$

Getting the exact value of λ_1 we find the following result for λ_2

$$\lambda_2 = -\frac{[-\alpha_q + 4\lambda_1(D-1) + (D-2)]}{2}. \quad (148)$$

With the values of λ_1 and λ_2 found, we then have c_1 and c_2 as $c_1 = \frac{(D-2)}{2}$ and $c_2 = \frac{(D-2)^2}{4}$. This leads to the solution $\psi = e^{\frac{(D-2)A}{4}}$. We see that it is independent of the q-form. The value of ν is $\nu^2 = \left(\frac{D-1}{2}\right)^2$. If $D = 5$ we always get $\nu = 2$. This is the reason why we get the same parameters for the gauge and Kalb-Ramond fields. The effective action for the zero mode of the q-form is

$$S_{eff} = -\frac{1}{2(q+1)!} \int e^{(D-2)A} dz \int d^A x \hat{F}_{\mu_1 \mu_2 \dots \mu_{q+1}}^T \hat{F}_T^{\mu_1 \mu_2 \dots \mu_{q+1}}. \quad (149)$$

Which tells us that we have a localized zero mode of the q-form for $D > 3$.

To help the reader to follow our paper, we made a table that organize all the values of first mass modes for both dispersion relation.

Table 3: Values of mass

ν	Field	Mass for (58) $10^{10}mm^{-1}$	Mass for the old relation $10^{10}mm^{-1}$
0.5	Kalb Ramond(KB) with dilaton	1.4	2.4
1	Gauge and KB free	0.7	2.7
1.5	Gauge coupled with Ricci scalar	0.16	3.4
1.84	Gauge with dilaton	0.05	3.8
2	Gauge and KB with both couplings, free gravitational and scalar	0.028	4
2.5	Gravitational with dilaton and KB With Ricci scalar	0.004	4.4
3	Gauge coupled with Ricci tensor	0.0005	5.5
3.17	Scalar with dilaton	0.00025	5.75
4	KB coupled with Ricci tensor	0.000006	7

7 Conclusion

In this paper, we studied the behavior of bosonic fields in the crystal manifold background. We revised the works [29,35] where we found some mistakes in the calculations of the dispersion relation, what leads to incorrect band gap structures. We then show how to get the correct dispersion relation and compare our results with the previous ones. The study is made for the scalar, gravitational, gauge, Kalb-Ramond and q-form fields, with and without the dilaton coupling. As new cases, we also introduced in this same background the geometrical coupling, and studied the gauge, Kalb-Ramond and q-form fields.

First we revisited the gravity case. The expression for the mass gap was first found in Ref. [29]. By using an heuristic reasoning they argue that the first allowed mass should be given by $m_{gap} = \mathcal{O}(1)/(l + L)$. However, using our numerical calculation with the original expression of Ref. [29], Eq. (13), we show in Fig. 2 that this numerator is (≈ 4). This value is about 150 times bigger than the first mass mode found using the correct dispersion relation (42), that is $m = 0.028/(l + L)$. As our first mass mode is much small compared with the first one found using (13), the correction in the Newton's law, in our case, is bigger than the previous one. Once that we consider a Yukawa like potential, the correction depends on an exponential. In our case, this exponential is $e^{-2.8x10^8 r}$, and the previous result leads to $e^{-4x10^{10} r}$. In addition, the correction in our case is due just to the first mass mode, while the result found in [29], is calculated considering all the mass modes in the Bulk. They perform the integral since the m_{gap} until infinity, this is not correct because the mass modes are not continuous, there is a gap between each allowed mass mode as we can see in Fig3.

Next we revisit the q-form fields in crystal manifold, first studied in Ref. [35]. The authors based their result in the wrong expression found previously by Kaloper et al [29]. Here we find the correct expression and compute the new mass bands for all the cases considered in Ref. [35]. The scalar and gravitational fields have the same dispersion relation due to the fact that both have $\nu = 2$ and therefore the conclusions are the same. However, for the free gauge field we find a completely different mass band. The comparison is shown in Fig. 6. The wrong dispersion relation leads to a numerical result that the first mass mode is $m = 2.7/(l + L)$, while our dispersion leads to $m = 0.7/(l + L)$ i.e about four times smaller. Another important aspect is that the previous mass band was very uncommon and any analogy or comparison with condensed matter was impossible.

The correct result is in complete agreement and very similar to the results found by the Kronig-Penney model. This similarity allow us to look for other similar effects that can be found in the crystal manifold. The Kalb-Ramond and gauge fields have the same mass dispersion due to the property of the Bessel functions. Next we revisit the q-forms coupled to with the dilaton. With the corrected dispersion relation at hand, we show that it is different for all the fields. This implies a different band gap structure. The analyses for the q-form field also changes. In the work [35], they said that it is possible to generate or suppress mass modes by controlling the dilaton coupling. According to our results it is not true. For all the cases studied one is very interesting and deserves special attention: the band gap structure of the Kalb-Ramond field coupled with the dilaton. It is the only one that is linear for the values of q considered. In that way, it is the unique that does not show a gap between the mass band. Another interesting fact is that, using the correct dispersion relation, the mass of the first mode decreases due to the presence of the dilaton, while that for the old dispersion, the masses increases as can be seen in table (3).

For the case of the geometrical coupling we see that when both of parameters are different of zero, we get the same results that for the free scalar and gravitational fields. When one of the parameters are turned off we get different results. For the couple of the KB and gauge field with the Ricci scalar the parameter ν is respectively 2.5 and 1.5. For the couple of this two fields with the Ricci tensor the values of ν are $\nu = 3$ for the gauge, and $\nu = 4$ for the KB. All the values of mass in this configuration can also be found in table(3). An interesting result is that we found a massive photon with mass given by $6.2 \times 10^{-31} \text{ kg}$ this is above the lower bound limit imposed experimentally [53]. When we generalize to the q-form case, we see that the parameter ν is $\nu^2 = (\frac{D-1}{2})^2$. Then, if $D = 5$ the result will always be $\nu = 2$. This is why we got $\nu = 2$ for the scalar, gauge and Kalb-Ramond fields. As future work we intent to study fermions in this background.

Acknowledgments

The authors would like to thank Alexandra Elbakyan and sci-hub, for removing all barriers in the way of science, and to Makarius Tahim for useful conversations. We acknowledge the financial support provided by the Conselho Nacional de Desenvolvimento Científico e Tecnológico (CNPq) and Fundação Cearense de Apoio ao Desenvolvimento Científico e Tecnológico (FUNCAP) through PRONEM PNE0112- 00085.01.00/16

References

- [1] R. de L. Kronig and W.G.Penney "Quantum Mechanics of Electrons in Crystal Lattices" Royal Society. 130,814 pp.499-513,(1931)<https://royalsocietypublishing.org/doi/abs/10.1098/rspa.1931.0019>
- [2] Bloch Z.Physik,vol.52,p.555(1928) <http://www.pwein.at/physics/Lectures/Famous-Papers/Z-Physik-52-555-1928.pdf>
- [3] L. Randall and R. Sundrum, Phys. Rev. Lett. **83**, 3370 (1999) doi:10.1103/PhysRevLett.83.3370 [hep-ph/9905221].<https://arxiv.org/abs/hep-ph/9905221>
- [4] L. Randall and R. Sundrum, Phys. Rev. Lett. **83**, 4690 (1999) doi:10.1103/PhysRevLett.83.4690 [hep-th/9906064].<https://arxiv.org/abs/hep-th/9906064>
- [5] A. Kehagias and K. Tamvakis, Phys. Lett. B **504**, 38 (2001) doi:10.1016/S0370-2693(01)00274-X [hep-th/0010112].<https://arxiv.org/abs/hep-th/0010112>
- [6] A. E. R. Chumbes, J. M. Hoff da Silva and M. B. Hott, Phys. Rev. D **85**, 085003 (2012) doi:10.1103/PhysRevD.85.085003 [arXiv:1108.3821 [hep-th]].<https://arxiv.org/abs/1108.3821>
- [7] Z. H. Zhao, Y. X. Liu and Y. Zhong, Phys. Rev. D **90**, no. 4, 045031 (2014) doi:10.1103/PhysRevD.90.045031 [arXiv:1402.6480 [hep-th]].<https://arxiv.org/abs/1402.6480>
- [8] B. Bajc and G. Gabadadze, Phys. Lett. B **474**, 282 (2000) doi:10.1016/S0370-2693(00)00055-1 [hep-th/9912232].<https://arxiv.org/abs/hep-th/9912232>
- [9] K. Ghoroku and A. Nakamura, Phys. Rev. D **65**, 084017 (2002) doi:10.1103/PhysRevD.65.084017 [hep-th/0106145].<https://arxiv.org/abs/hep-th/0106145>
- [10] G. Alencar, R. R. Landim, M. O. Tahim and R. N. Costa Filho, Phys. Lett. B **739**, 125 (2014) doi:10.1016/j.physletb.2014.10.040 [arXiv:1409.4396 [hep-th]].<https://arxiv.org/abs/1409.4396>

- [11] Z. H. Zhao, Q. Y. Xie and Y. Zhong, *Class. Quant. Grav.* **32**, no. 3, 035020 (2015) doi:10.1088/0264-9381/32/3/035020 [arXiv:1406.3098 [hep-th]].<https://arxiv.org/abs/1406.3098>
- [12] I. Oda, *Phys. Lett. B* **508**, 96 (2001) doi:10.1016/S0370-2693(01)00376-8 [hep-th/0012013].<https://arxiv.org/abs/hep-th/0012013>
- [13] R. I. De Oliveira Junior, M. O. Tahim, G. Alencar and R. R. Landim, *Mod. Phys. Lett. A* **35**, no. 08, 2050047 (2019) doi:10.1142/S0217732320500479 [arXiv:1902.10669 [hep-th]].<https://arxiv.org/abs/1902.10669>
- [14] L. F. Freitas, G. Alencar and R. R. Landim, *JHEP* **1902**, 035 (2019) doi:10.1007/JHEP02(2019)035 [arXiv:1809.07197 [hep-th]].<https://arxiv.org/abs/1809.07197>
- [15] W. M. Mendes, G. Alencar and R. R. Landim, *JHEP* **1802**, 018 (2018) doi:10.1007/JHEP02(2018)018 [arXiv:1712.02590 [hep-th]].<https://arxiv.org/abs/1712.02590>
- [16] D. Bazeia, A. R. Gomes and L. Losano, *Int. J. Mod. Phys. A* **24**, 1135 (2009) doi:10.1142/S0217751X09043067 [arXiv:0708.3530 [hep-th]].<https://arxiv.org/abs/0708.3530>
- [17] R. C. Fonseca, F. A. Brito and L. Losano, *Phys. Lett. B* **728**, 443 (2014) doi:10.1016/j.physletb.2013.12.020 [arXiv:1211.0531 [hep-th]].<https://arxiv.org/abs/1211.0531>
- [18] M. S. Cunha and H. R. Christiansen, *Phys. Rev. D* **84**, 085002 (2011) doi:10.1103/PhysRevD.84.085002 [arXiv:1109.3486 [hep-th]].<https://arxiv.org/abs/1109.3486>
- [19] C. A. S. Almeida, M. M. Ferreira, Jr., A. R. Gomes and R. Casana, *Phys. Rev. D* **79**, 125022 (2009) doi:10.1103/PhysRevD.79.125022 [arXiv:0901.3543 [hep-th]].<https://arxiv.org/abs/0901.3543>
- [20] Y. X. Liu, J. Yang, Z. H. Zhao, C. E. Fu and Y. S. Duan, *Phys. Rev. D* **80**, 065019 (2009) doi:10.1103/PhysRevD.80.065019 [arXiv:0904.1785 [hep-th]].<https://arxiv.org/abs/0904.1785>
- [21] Y. X. Liu, H. T. Li, Z. H. Zhao, J. X. Li and J. R. Ren, *JHEP* **0910**, 091 (2009) doi:10.1088/1126-6708/2009/10/091 [arXiv:0909.2312 [hep-th]].<https://arxiv.org/abs/0909.2312>
- [22] W. T. Cruz, M. O. Tahim and C. A. S. Almeida, *EPL* **88**, no. 4, 41001 (2009) doi:10.1209/0295-5075/88/41001 [arXiv:0912.1029 [hep-th]].<https://arxiv.org/abs/0912.1029>
- [23] Z. H. Zhao, Y. X. Liu, H. T. Li and Y. Q. Wang, *Phys. Rev. D* **82**, 084030 (2010) doi:10.1103/PhysRevD.82.084030 [arXiv:1004.2181 [hep-th]].<https://arxiv.org/abs/1004.2181>

- [24] H. T. Li, Y. X. Liu, Z. H. Zhao and H. Guo, Phys. Rev. D **83**, 045006 (2011) doi:10.1103/PhysRevD.83.045006 [arXiv:1006.4240 [hep-th]].<https://arxiv.org/abs/1006.4240>
- [25] W. T. Cruz, A. R. Gomes and C. A. S. Almeida, EPL **96**, no. 3, 31001 (2011) doi:10.1209/0295-5075/96/31001 [arXiv:1110.3104 [hep-th]].<https://arxiv.org/abs/1110.3104>
- [26] R. Landim, G. Alencar, M. Tahim and R. Costa Filho, JHEP **08**, 071 (2011) doi:10.1007/JHEP08(2011)071 [arXiv:1105.5573 [hep-th]].<https://arxiv.org/abs/1207.3054>
- [27] R. R. Landim, G. Alencar, M. O. Tahim and R. N. Costa Filho, JHEP **1202**, 073 (2012) doi:10.1007/JHEP02(2012)073 [arXiv:1110.5855 [hep-th]].<https://arxiv.org/abs/1110.5855>
- [28] G. Alencar, R. R. Landim, M. O. Tahim and R. N. C. Filho, JHEP **1301**, 050 (2013) doi:10.1007/JHEP01(2013)050 [arXiv:1207.3054 [hep-th]].<https://arxiv.org/abs/1207.3054>
- [29] N. Kaloper, Phys. Lett. B **474**, 269 (2000) doi:10.1016/S0370-2693(00)00028-9 [hep-th/9912125].<https://arxiv.org/abs/hep-th/9912125>
- [30] N. Kaloper, JHEP **0405**, 061 (2004) doi:10.1088/1126-6708/2004/05/061 [hep-th/0403208].<https://arxiv.org/abs/hep-th/0403208>
- [31] I. Oda, Phys. Lett. B **480**, 305 (2000) doi:10.1016/S0370-2693(00)00392-0 [hep-th/9908104].<https://arxiv.org/abs/hep-th/9908104>
- [32] S. Nam, JHEP **0003**, 005 (2000) doi:10.1088/1126-6708/2000/03/005 [hep-th/9911104].<https://arxiv.org/abs/hep-th/9911104>
- [33] S. Nam, JHEP **0004**, 002 (2000) doi:10.1088/1126-6708/2000/04/002 [hep-th/9911237].<https://arxiv.org/abs/hep-th/9911237>
- [34] A. Papazoglou, hep-ph/0112159.<https://arxiv.org/abs/hep-ph/0112159>
- [35] G. Alencar, R. R. Landim, M. O. Tahim and R. N. Costa Filho, Phys. Lett. B **726**, 809 (2013) doi:10.1016/j.physletb.2013.09.006 [arXiv:1301.2562 [hep-th]].<https://arxiv.org/abs/1301.2562>
- [36] J. Khoury, B. A. Ovrut, P. J. Steinhardt and N. Turok, Phys. Rev. D **64**, 123522 (2001) doi:10.1103/PhysRevD.64.123522 [hep-th/0103239].<https://arxiv.org/abs/hep-th/0103239>
- [37] M. Majumdar and A. Christine-Davis, JHEP **0203**, 056 (2002) doi:10.1088/1126-6708/2002/03/056 [hep-th/0202148].<https://arxiv.org/abs/hep-th/0202148>

- [38] R. Foot, Int. J. Mod. Phys. A **29**, 1430013 (2014) doi:10.1142/S0217751X14300130 [arXiv:1401.3965 [astro-ph.CO]].<https://arxiv.org/abs/1401.3965>
- [39] L. Bergström, Rept. Prog. Phys. **63**, 793 (2000) doi:10.1088/0034-4885/63/5/2r3 [hep-ph/0002126].<https://arxiv.org/abs/hep-ph/0002126>
- [40] G. Alencar, R. R. Landim, M. O. Tahim, K. C. Mendes and R. N. Costa Filho, EPL **93**, no. 1, 10003 (2011) doi:10.1209/0295-5075/93/10003 [arXiv:1009.1183 [hep-th]].<https://arxiv.org/abs/1009.1183>
- [41] B. Mukhopadhyaya, S. Sen, S. Sen and S. SenGupta, Phys. Rev. D **70**, 066009 (2004) doi:10.1103/PhysRevD.70.066009 [hep-th/0403098].<https://arxiv.org/abs/hep-th/0403098>
- [42] A. Arvanitaki, S. Dimopoulos, S. Dubovsky, N. Kaloper and J. March-Russell, Phys. Rev. D **81**, 123530 (2010) doi:10.1103/PhysRevD.81.123530 [arXiv:0905.4720 [hep-th]].<https://arxiv.org/abs/0905.4720>
- [43] P. Svrcek and E. Witten, JHEP **0606**, 051 (2006) doi:10.1088/1126-6708/2006/06/051 [hep-th/0605206].<https://arxiv.org/abs/hep-th/0605206>
- [44] B. Mukhopadhyaya, S. Sen and S. SenGupta, Phys. Rev. D **76**, 121501 (2007) doi:10.1103/PhysRevD.76.121501 [arXiv:0709.3428 [hep-th]].<https://arxiv.org/abs/0709.3428>
- [45] J. Polchinski, "String theory. Vol.1: An introduction to the bosonic string". SPIRES entry Cambridge ,UK: Univ.Pr.(1998) 402 p.
- [46] J. Polchinski, "String theory. Vol.2: An introduction to the bosonic string". SPIRES entry Cambridge ,UK: Univ.Pr.(1998) 531 p.
- [47] M. Kulaxizi and R. Rahman, JHEP **1410**, 193 (2014) doi:10.1007/JHEP10(2014)193 [arXiv:1409.1942 [hep-th]].<https://arxiv.org/abs/1409.1942>
- [48] G. Alencar, I. Jardim and R. Landim, Eur. Phys. J. C **78**, no.5, 367 (2018) doi:10.1140/epjc/s10052-018-5829-6 [arXiv:1801.06098 [hep-th]].<https://arxiv.org/abs/1801.06098>
- [49] G. Alencar, I. Jardim, R. Landim, C. Muniz and R. N. Costa Filho, Phys. Rev. D **93**, no.12, 124064 (2016) doi:10.1103/PhysRevD.93.124064 [arXiv:1506.00622 [hep-th]].<https://arxiv.org/abs/1506.00622>
- [50] I. Jardim, G. Alencar, R. Landim and R. Costa Filho, JHEP **04**, 003 (2015) doi:10.1007/JHEP04(2015)003 [arXiv:1410.6756 [hep-th]].<https://arxiv.org/abs/1410.6756>

- [51] G. Alencar, R. Landim, M. Tahim and R. Costa Filho, Phys. Lett. B **742**, 256-260 (2015) doi:10.1016/j.physletb.2015.01.041 [arXiv:1409.5042 [hep-th]].<https://arxiv.org/abs/1409.5042>
- [52] R. R. Landim, G. Alencar, M. O. Tahim, M. A. M. Gomes and R. N. Costa Filho, EPL **97**, no. 2, 20003 (2012) doi:10.1209/0295-5075/97/20003 [arXiv:1010.1548 [hep-th]].<https://arxiv.org/abs/1010.1548>
- [53] C. Patrignani *et al.* [Particle Data Group], Chin. Phys. C **40**, no.10, 100001 (2016) doi:10.1088/1674-1137/40/10/100001<https://inspirehep.net/files/a46bc344915850ae75930afef3e5b526>